Journal of *Marine Science and Engineering*

MDPI

Article

Benthic Foraminifera and Productivity Regimes in the Kveithola Trough (Barents Sea)—Ecological Implications in a Changing Arctic and Actuopaleontological Meaning

Anna Sabbatini [1,*], Matteo Bazzaro [2], Francesca Caridi [1], Cinzia De Vittor [2], Valentina Esposito [2], Renata Giulia Lucchi [2], Alessandra Negri [1] and Caterina Morigi [3]

[1] Dipartimento di Scienze della Vita e dell'Ambiente, Università Politecnica delle Marche, Via Brecce Bianche, 60131 Ancona, Italy
[2] National Institute of Oceanography and Applied Geophysics—OGS, 34010 Trieste, Italy
[3] Dipartimento di Scienze della Terra, Università di Pisa, Via Santa Maria, 53, 56126 Pisa, Italy
* Correspondence: a.sabbatini@univpm.it; Tel.: +39-3288185182

Abstract: The rapid response of benthic foraminifera to organic carbon flux to the seafloor makes them promising bioindicators for evaluating the organic carbon stored in marine sediments. Fjords have been described as hotspots for carbon burial, potentially playing a key role within the carbon cycle as climate regulators over multiple timescales. Nevertheless, little is known about organic carbon-rich sediments in Arctic open shelves and their role in global carbon sequestration. To this aim, four sites have been sampled along a W-E transect across the Kveithola Trough located in the NW Barents Sea. Living (stained) benthic foraminiferal density, biodiversity and vertical distribution in the sediment were analysed together with the biogeochemical and sedimentological data. We identified two main depositional environments based on the relationship between benthic foraminiferal assemblages and carbon content in the sediments: (1) an oligotrophic land-derived organic matter region located in the outer part of the trough influenced by the warm and saline Atlantic Water; and (2) a stressed eutrophic environment, with high-content of metabolizable organic matter in the inner part of the trough, which comprises the main drift and the Northern flank of the trough. The freshness and good nutritional quality of the organic matter detected in the inner region could be the result of the better preservation of the organic matter itself, basically driven by the rapid burial of fine-grained organic-rich sediments enhanced by the cold and less saline Arctic Water coming from the Barents Sea. We conclude that foraminifera provide a tool to describe the Kveithola depositional environment as a carbon burial hotspot in a changing Arctic area subjected to a pulse of fresh food intended as biopolymeric carbon.

Keywords: benthic foraminifera; Kveithola trough; Barents Sea; arctic; sedimentary organic matter; biopolymeric carbon; suboxic conditions

Citation: Sabbatini, A.; Bazzaro, M.; Caridi, F.; De Vittor, C.; Esposito, V.; Lucchi, R.G.; Negri, A.; Morigi, C. Benthic Foraminifera and Productivity Regimes in the Kveithola Trough (Barents Sea)—Ecological Implications in a Changing Arctic and Actuopaleontological Meaning. *J. Mar. Sci. Eng.* **2023**, *11*, 237. https://doi.org/10.3390/jmse11020237

Academic Editor: Dmitry A. Ruban

Received: 5 December 2022
Revised: 11 January 2023
Accepted: 12 January 2023
Published: 17 January 2023

1. Introduction

The Barents Sea is a marginal area of the Arctic Ocean, and it represents a rather shallow shelf sea, with an average depth of 230 m. It is a complex and dynamic oceanographic area, being partly ice-free during winter in the present climate. Although it constitutes about 10% of the Arctic Ocean, it occupies a key position on the eastern side of the main gateway between the Arctic and the Atlantic Oceans. Hydrologic changes, due to global warming, have led recently to a reduction in sea ice, in stratification of the water column and high seasonal and inter-annual variability, which have large effects on the marine ecosystem and environment [1,2]. The Barents Sea and Svalbard waters are highly productive provinces accounting for 49% of the total Arctic shelf primary production [3]. In particular, the total annual primary production for the Barents Sea has been estimated to be around 70–100 g C/m^{-2} with higher rates for the open Atlantic waters in the southern parts

and lower rates for the ice-covered waters in the northern Barents Sea [4]. High primary production rates are bound to regions that are under the influence of advected Atlantic Water, while ice-covered regions and those stratified by Arctic Water experience reduced rates. Furthermore, primary production is strongly dependent upon light availability and the presence of nutrients. In the Arctic region and its adjacent shelf seas, primary production is highly seasonal (late spring) due to the melting and retreat of the sea ice during spring, which enhance light and nutrients availability driving the growth of the algae [5,6].

During the last 15 years, the Arctic region has undergone an important increase of primary production, especially close to the inner continental shelves [7]. Statistically, significant increasing trends of primary productivity from 2003 to 2015 occurred in the eastern (Eurasian) Arctic, Barents Sea, Greenland Sea, and North Atlantic with particularly high increases in the eastern Arctic (19.26 g $C/m^2/yr/dec$, 41.9% increase) and the Barents Sea (17.98 g $C/m^2/yr/dec$, 30.2% increase) [8]. There is increasing attention to how climate changes can influence productivity and ecosystems in Arctic regions. Changing sea ice conditions and distribution influence stratification and upwelling, enhancing wind exposure, with an effect on nutrient supply and productivity [9,10].

In the melting Arctic, seasonal organic matter export to the seafloor can provoke temporal and strong episodic events of anoxia [11]. Several studies have provided evidence that eutrophication, considered as a high accumulation of labile organic matter, is associated with a net accumulation or burial of organic carbon in the sediment [12–14] determining changes in the benthic trophic status [15]. Furthermore, labile organic carbon concentrations have been demonstrated to be positively correlated to the sediment oxygen consumption promoted by benthic consumers, suggesting that the progressive burial of biopolymeric carbon could be an additional co-factor potentially responsible for hypoxic or anoxic events [15].

In this context, there is, therefore, an urgent necessity to deepen knowledge on the present environmental setting because the Barents Sea is home to an enormous diversity of organisms, which are experiencing climatic variability and, among them, foraminifera represent a lower trophic level group [16]. Foraminifera are unicellular eukaryotes that occur ubiquitously in all the world oceans and in all marine habitats, including both pelagic and benthic environments. Benthic foraminifera are one of the main components of marine ecosystems [17]. They are characterised by a short life cycle (when compared to macrofaunal metazoans) and react rather quickly to both short and long-term changes in marine and transitional-marine environments on both a global and a local scale [18]. For these reasons, foraminifera are used increasingly to evaluate the environmental status of marine shelf systems impacted by pollution and eutrophication [19–22]. Therefore, benthic foraminifera are potentially good indicators of the benthic trophic conditions in terms of nutritionally available organic matter and, indirectly, of oxygen consumption [21,23].

As matter of fact, temporal and strong episodic events of anoxia are stressful to most organisms, also to the benthic foraminifera, which play an important role in maintaining the carbon budget to the seafloor [24]. The vertical distribution of benthic foraminifera across the first 10 cm sediment depth mainly depends on two inversely related drivers, the organic matter accumulation to the seafloor (usually fresh food of high nutritional values at the sediment-water interface) and decreasing concentration of oxygen in the sediment porewater [23,25,26].

The ability of foraminifera in taking up fresh carbon for nutrition and reproduction varies depending on species and areas [27,28]. Studies indicate that labile organic matter entering the benthic environment can be rapidly processed within hours [29–31] and that some foraminifera play an important role in the carbon cycle [24]. At the same time, some species show a strong tolerance to hypoxia and proliferate in oxygen-depleted environments [32–36]. The authors of [37,38] show that *Globobulimina affinis* lives in anoxic sediments, indicating survival in depleted oxygen conditions other taxa may not tolerate. Specimens belonging to the genera *Bolivina*, *Globobulimina*, *Nonionella*, *Nonionellina* and *Stainforthia* are considered foraminifera inhabiting oxygen-depleted environments able to survive in closed basins with

high anthropogenic organic load and/or seasonal eutrophic settings [34]. In this regard, various mechanisms explain how foraminifera survive in these adverse conditions and these include anaerobic metabolic pathways, bacterial symbionts, chloroplasts sequestration or proliferation of peroxisomes and mitochondria, up to the ability of some calcareous foraminifera to use nitrate for respiration instead of oxygen ([39–41] and references therein). At present, many of the studies cited above show that oxygen concentration and organic matter quality and quantity drive the density and taxonomic composition of foraminiferal assemblages. However, due to the inverse relationship of food vs. oxygen availability, their relative importance remains difficult to resolve. The existing living benthic foraminiferal-based reports in the Barents Sea are limited to a few studies [16,42–45] mainly dealing with the use of recent assemblages to interpret late Quaternary paleoenvironmental changes [46,47] or combining live and total assemblage in tracking environmental changes [44,48]. The extensive data on past foraminiferal assemblages in the Barents Sea is reported in [49,50] database retrieved from the following sources: [51–56]. Most of the data on living benthic foraminiferal populations are from the fjords of Svalbard [57,58], in particular, in relation to environmental gradients but a comprehensive investigation of their distribution in response to organic carbon currently stored in the Arctic shelf sediments is still missing. In this context, the aim of this study are: (1) to describe, the living benthic foraminiferal assemblage collected from 4 different depositional settings in a shelf depression in the NW Barents Sea, namely the Kveithola Trough; this also include mapping the density and biodiversity of living benthic foraminifera, including the monothalamous component, representing in other shallower Arctic sites more than 50% of the total assemblage [59]; (2) to determine how quantity, quality, and composition of the organic matter (in terms of Total Organic Carbon, Total Nitrogen and biopolymeric carbon, defined as the sum of protein, lipid, carbohydrate, *sensu* [60]) drive the abundance and vertical distribution of living benthic foraminifera in the area; and (3) we put emphasis on the actuopaleontology as an useful approach for past reconstructions. Actuopaleontology is a modern discipline using an actualistic approach; it aims to improve our understanding of the past buried in the fossil record by studying the patterns and processes observed in the present. In other words, the present is used as the key to the past considering that physical, biological, and ecological processes in the past must have been similar to those occurring in our current environment. Finally, the present work aims to describe the benthic foraminiferal living Rose Bengal-stained assemblage in the Kveithola Trough three years before respect to the previous paper in the same area [16]. In 2016 samples, the Cell Tracker Green staining method was used to distinguish between dead and living specimens. The focus of the present work is mainly to understand the response of foraminifera to food quantity and quality in the sediment (0–10 cm) and [16] provided a set of environmental drivers that include organic matter analyses in the superficial sediment samples (0–2 cm).

2. Materials and Methods

2.1. Study Area: The Kveithola Trough

The Kveithola Trough has been surveyed during several cruises (the following oceanographic expeditions: EGLACOM (Evolution of a GLacial Arctic COntinental Margin: the southern Svalbard ice stream-dominated sedimentary system), Italian R/V OGS-Explora, 8 July–4 August 2008; GlaciBar (Glaciations in the Barents Sea area; 200672/S60), Norwegian R/V Jan Mayen, 2–19 July 2009; MSM30-CORIBAR (Ice dynamics and meltwater deposits: coring in the kveithola trough, NW Barents Sea), German R/V Maria S. Merian, 16 July–15 August 2013, Tromsø (Norway)—Tromsø (Norway) and PS99-1a, Eurofleets2-BURSETER (Bottom Currents in a Stagnant Environment), German R/V Polarstern, 13–23 June 2016, Bremerhaven (D)—Longyearbyen (NOR)) focusing mainly on the glacial history of the area associated to climate changes. Our study is focalized on this glacigenic depression located in the NW Barents Sea, north of Bear Island, an abrupt and narrow trough that hosted ice streams during Last Glacial Maximum (LGM) [61–63] (Figure 1). The Kveithola Trough is nearly 90 km long from the shelf edge to its eastward termination, and less than 15 km wide and has water depths between 300 and 350 m along

its axis. On regional bathymetric data (Figure 1) compiled by the Norwegian Hydrographic Service [64], the Kveithola Trough shows a very fresh morphology terminating abruptly eastward at the divide between the Spitsbergen Bank and Bear Island topographic highs (Figure 1).

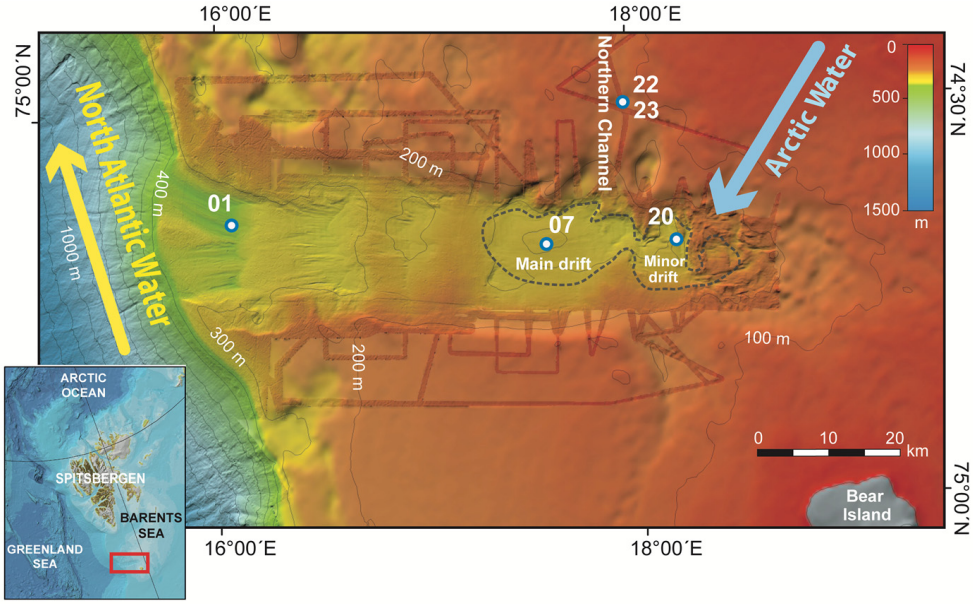

Figure 1. Bathymetric map of the Kveithola Trough in the Barents Sea and sampling sites. Dotted lines evidence the outer and inner areas of the Kveithola Trough that are deeper and shallower than 300 m wd, respectively. The inset indicates the studied area located south of Svalbard. This figure modified after Figure 1 in [16].

The transverse profile of the trough is U-shaped with flanks dipping about 2° and a flat thalweg, about 150 m below the average depth of the continental shelf seafloor in which it is incised. The axial profile is gently dipping ocean-wards from 200 to 400 m bsl (below sea level), having a step-like longitudinal profile as result of a spasmodic ice stream retreat after LGM that generated transversal depositional ridges (Grounding Zone Wedges—GZW, *sensu* [65], along the retreating palaeo-grounding line. The inner part of the trough hosts a complex sediment drift characterized by two main depocentres (main and minor drifts; [66]) (Figure 1), with internal acoustic reflectors on the sub-bottom record indicating persistent bottom currents that were active in the area since at least 13,000 calibrated years before present (cal Ka BP; [63,66]). The dataset recovered during the cruises outlined a highly dynamic depositional environment with strong bottom currents responsible for sediment drifts formation [67]. Beside of the highly dynamic depositional environment, depicted from the morphological and structural characteristics of the sediment drift [66] the lithofacies characteristics of surface sediments indicate, in the inner part, low-energy and/or low-oxygen conditions with black sediments containing hydrogen sulfide [68]. On the outer trough, at only a few tens of km distance, the sediments appear fully oxygenated, characterized by fine-grained, clean sands at the sea surface with large scale ripple-like features suggesting the presence of moderately strong and persistent bottom currents.

Two main water masses determine the present oceanographic situation in the study area, Atlantic Water and Arctic Water (Figure 1). The North Atlantic Water intrudes eastward where the Barents Sea continental shelf is dissected by troughs (Figure 1). The cold and less saline Arctic Water enters the western Barents Sea from the northeast and occupies large parts of the Barents Sea (Figure 1; [69]). As reported by [16] the Kveithola Trough is a peculiar geomorphological area characterised by a large portion of relatively shallow seabed, where the water column is strongly influenced by the co-presence and interplay of the Arctic water masses, seasonal influence of sea-ice melting waters, and atmospheric processes able to induce local water mass mixing and enhance a strong spatial

and temporal variability of the thermohaline properties. Moreover, it is similar to other Barents Sea shallow areas, where high nutrient fluxes reach the benthic community and high regional primary and secondary production exist [70–72].

2.2. Sampling Strategy

Five out of 14 sites cored in the Kveithola Trough during the oceanographic expedition MSM30-CORIBAR (Ice dynamics and meltwater deposits: coring in the Kveithola trough, NW Barents Sea), German R/V Maria S. Merian, 16.07–15.08.2013, Tromsø (Norway)—Tromsø (Norway), were selected for the sediment analyses presented in this paper (Figure 1; Table 1).

Table 1. Position data. Multiple deployments are indicated with consecutive numbers after the name of the site.

Cruise	Site	Sea Floor Morphology	Coordinates	Water Depth (m)	Analyses
GeoB176	01	Grounding-Zone Wedges (GZW)	74°51.53′ N 16°05.81′ E	371	Foraminifera, sediment, biochemistry
	07	Main drift	74°50.74′ N 17°38.35′ E	298	Foraminifera, sediment, biochemistry
	20	Minor drift	74°50.74′ N 18°10.53′ E	333	Foraminifera, sediment, biochemistry
	22	Northern Channel	74°59.69′ N 17°59.59′ E	167	Foraminifera sediment
	23		75° 0.46′ N 17° 58.85′ E	150	Biochemistry

Site 01 was located on the outermost Grounding Zone Wedge (GZW); site 07 and site 20 were situated on the main and minor Kveithola drifts, respectively; sites 22 and 23 were located north of the Kveithola Trough along a NNE-SSW depression associated with the regional fault system that will be called Northern channel.

The cores were retrieved using both a multi-corer sampling tool (MUC) allowing the recovery of undisturbed surface sediment samples with eight plastic liners measuring 6 cm in diameter and 50 cm in length; and a giant box-corer (GBC) with a 50 cm × 50 cm × 50 cm steel box. Sediment surfaces were visually described during the cruise and one of the sub-sampled cores collected from each box-corer was opened and visually logged onboard for sedimentological characteristics and preliminary stratigraphy [68]. Cores, from both MUC and GBC, were collected for sedimentological and biochemical analyses and living foraminiferal assemblage investigation as indicated in Table 1. Sediment material from site 22 was sub-sampled for foraminiferal and sedimentological analyses and from site 23 for biochemical determinations. Biochemical data of site 23 are comparable to those recorded in site 07 collected in the Kveithola Trough 3 years later (Expedition PS99-1a), and site 07 ([16] see Table 1 therein) corresponds to Site 22 of this study (see Table 1 therein). Then considering that these sampling sites are all located in the Northern channel we assume that the biochemical signature of site 22 does not differ from those in site 23.

2.3. Sedimentological Analyses

Sedimentological analyses (sites 01, 07, 20 and 22) were run using both automated core-logging techniques with sampling measurements at 1 cm resolution and traditional analytical methods on discrete samples. Core-scanning included: a Computed Tomography scan (CAT-scan) radiographs performed prior to core opening; high-resolution digital photographs, color scan, and chemical composition of the sediments by means of an Avaatech Superslit X-Ray-Fluorescence core scan (XRF-core scan) using 10, 30, and 50 kV instrumental settings.

Discrete sediment samples were collected at every 10–5 cm resolution and analyzed for sediment physical properties and composition. Grain size analyses were performed with a Coulter counter laser Beckman LS-230 to measure the 0.04–2000 µm fraction at 0.004 µm resolution. The samples were initially treated with 10-volume diluted peroxide and the dis-aggregated sediments were re-suspended into a 0.1% sodium-hexametaphosphate solution and left for 3 min in an ultrasonic bath prior to measurement. The results were classified according to the Udden-Wentworth grain-size scale and were analyzed with the cluster statistical method.

2.4. Total Organic Carbon (TOC), Total Nitrogen (TN), and Biopolymeric Carbon (BPC)

Cores for biochemical analyses (sites 01, 07, 20 and 23) (Table 1) were stored frozen at −20 °C until processing at the on-land laboratory (Table 1). All the cores were sliced at 0.5 cm resolution down to 2 cm sediment depth and then every 1 cm down to 10 cm. Sediment samples were freeze-dried, homogenized and ground to a fine powder for analyses of Total Organic Carbon (TOC), Total Nitrogen (TN) and biopolymeric carbon (BPC, as the sum of carbohydrate (CHO), protein (PRT) and lipid (LIP) carbon). TOC and TN were measured using an elemental analyser CHNO-S Costech mod. ECS 4010 according to [73]. The sediment was weighed in subsamples of about 8–12 mg in triplicate on a micro ultra-balance Mettler Toledo mod. XP 6 (accuracy of 0.1 μg). For the analyses of the TOC, the subsamples were treated in silver capsules with the following addition of hydrochloric acid at increased concentration (0.1 N, 0.5 N and 1 N) to remove the carbonate fraction [74], whereas for the analyses of TN freeze-dried sediments were placed in tin capsules with no treatment. Known amounts of standard Acetanilide (C_8H_9NO; Costech, purity $\geq$ 99.5%) were used to calibrate the instrument. The accuracy of the method for total carbon was verified against the certified marine sediment reference material PACS-2 (National Research Council Canada). The relative standard deviations for three replicates determination of carbon on the CRM were lower than 3%.

Two different CHO fractions (water-soluble, CHO_{H2O} and EDTA-extractable, CHO_{EDTA}) were determined following [75]. The carbohydrate fractions were measured spectrophotometrically using the phenol-sulphuric acid assay [76], modified by [77] for sediment samples. CHO concentrations were calculated from calibration curves of D-glucose. CHO concentrations, obtained as equivalent-glucose, were transformed into carbon using a conversion factor of 0.49 g C g^{-1} [78].

Protein (PRT) analyses were carried out on freeze-dried sediment samples after extractions with NaOH (0.5 M, 4 h). PRT were determined according to [79] modified by [80] to compensate for phenol interference. PRT concentrations were calculated from calibration curves of serum albumin. Even if determination could be affected by the interference of humics [80], this method was chosen due to its ease and high sensitivity. Moreover, the wide application of this protocol makes our results comparable with other studies [15,78,81]. Concentrations obtained as albumin equivalents were transformed into carbon using a conversion factor of 0.50 g C g^{-1} [56]. Total lipids (LIP) were extracted by direct elution with chloroform and methanol following the procedure of [82] and analyzed according to [83]. LIP concentrations were calculated from calibration curves of tripalmitine. Concentrations obtained as tripalmitine equivalents were transformed into carbon using a conversion factor of 0.75 g C g^{-1} [60]. All biochemical analyses were carried out in 3–5 replicates, with a standard deviation lower than 5%. The sum of the carbon equivalents of CHO, PRT and LIP was referred to as BPC (*sensu* [60]). Contribution of protein to biopolymeric carbon (PRT/BPC%) and protein to carbohydrate ratio (PRT: CHO) were then used as descriptors of both ageing and nutritional quality of the organic matter [84–89].

2.5. Foraminiferal Analyses

Subsamples for foraminiferal analyses (sites 01, 07, 20 and 22) (Table 1) were obtained using Plexiglas cores, inner diameter 3.6 cm (surface area 10.18 cm^2) inserted manually in the MUC or GBC cast. Two cores (01 and 07) were sampled on board. The two remaining cores (20 and 22) were immediately stored at −20 °C until analyses in the laboratory. All the cores were sliced at 0.5 cm resolution down to 2 cm sediment depth and then every 1 cm down to 10 cm. The samples were stained with Rose Bengal solution (1 g L^{-1}) and preserved in 10% borax-buffered formalin following the protocol largely used for ecological study of meiofauna including foraminifera and soft-shelled taxa among foraminifera which will be partially destroyed using ethanol [90–92]. Sodium borate buffer is used to maintain the pH of formalin solution within a relatively narrow range in order to not cause the dissolution of foraminiferal calcitic shells.

In the laboratory, the fixed sediment samples were sieved through 63 and 150 μm mesh (in order to evaluate the size structure of foraminiferal assemblage) and preserved in 10% borax-buffered formalin to which had been added Rose Bengal (1 g L^{-1}). The residues were kept wet and hand-sorted in water for all Rose-Bengal-stained benthic foraminifera using a binocular microscope. Hard-shelled polythalamous foraminifera (agglutinated and calcareous species) were stored dried in micro-palaeontological slides and calcitic test preservation of most abundant species was random checked at Scanning Electron Microscope (SEM—Hitachi). Soft-shelled monothalamous taxa were placed in cavity slides in glycerol and photographed under a compound microscope (Nikon Eclipse E 600 POL). All the specimens were counted, and their numbers standardized per 10 cm^2 and if necessary, per 50 cm^2 to compare our results with the literature data. For the same reason, foraminifera from the small-size (63–150 μm) and the >150 μm fraction were investigated.

Rose Bengal is a cheap, easy and fast procedure, resulting useful for environmental sample analysis but it is well known to be not completely reliable for the staining of recently dead cells, because remnants of tissues may remain preserved (and thus stainable) for a long time within dead organisms [93]. As such, since the Rose Bengal binds proteins and other macromolecules, the potential for generating false positive cells is quite high especially in low oxygen settings where the cell material may persist long after death [38,94]. In order to minimize overestimation in the live foraminiferal counts, strict staining criteria were always applied. Specimens were considered "alive" only when all chambers, except for the last one, were well stained. A special effort was made to recognize soft-shelled monothalamous taxa, which are largely undescribed, and they are included in this data analyses. Fragments of branching and tubular foraminifera (e.g., *Hyperammina* and *Rhizammina*) were included in the data analyses only when it was possible to quantify them correctly (presence of proloculus) because of their easily breakable tests.

Species identification followed previous studies from the high latitude environments and for the hard-shelled polythalamous foraminifera (agglutinated and calcareous taxa) taxonomy we followed papers and atlas by [59,95–100]. For the soft-shelled monothalamous foraminifera taxonomy, we followed papers by [101–104].

Foraminiferal biodiversity was estimated using different diversity indices: species richness (S) measured as the number of species, species diversity (H loge) expressed as the Shannon–Wiener (H) index and species evenness (J) measured using the [105]. All indices were calculated using the statistical PAST software (Paleontological Statistics; Version 2.14; [106]) for all the levels and for the total 0–10 cm.

In order to describe the vertical distribution of the total assemblages or individual taxa, we used the average living depth (ALD, [107]), which allows a rapid description of the microhabitat patterns. The ALD is calculated according to the following equation:

$$\mathrm{ALDx} = \sum_{i=0,x} (niDi)/N$$

where x is the lower boundary of deepest sample, ni the number of individuals in interval i; Di the midpoint of sample interval i; N the total number of individuals for all levels. For all stations, ALD10 was calculated for the whole assemblage as well as for individual taxa and for both size fractions, on the basis of the numbers of stained individuals found in the successive sediment slices. In case of a strictly epifaunal taxon, the ALD should be one half of the thickness of the topmost level. Higher values are indicative of more infaunal patterns [107].

2.6. Statistical Analyses

To assess spatial variations of each investigated variable separately, one-way analyses of variance (ANOVA) was applied. The analyses considered the four sampling sites as random levels of the factor Space. To test spatial variations in the biochemical composition of sediment organic matter and the composition of the benthic foraminiferal assemblages, multivariate permutational analyses of variance (PERMANOVA [108]) based on Euclidean

and Bray–Curtis distances (for organic matter and foraminiferal assemblage, respectively) were applied. SIMPER analyses were applied to assess the dissimilarity percentage between foraminiferal assemblages in the four different sampling sites and to identify which species contributed most to the observed dissimilarities between sampling sites. ANOVA, PERMANOVA and SIMPER analyses were performed using the PAST software (Paleontological Statistics; Version 2.14; [106]).

Then multivariate analyses were performed in order to assess potential correlations between the foraminiferal assemblage and the biochemical components of the sedimentary organic matter (BPC, C-CHO$_{H2O}$, C-CHO$_{EDTA}$, C-PRT, C-LIP, TOC, TN, N-PRT/TN, TOC/TN), using the statistical software applications PRIMER6 & PERMANOVA+ [109,110]. Potential differences between biodiversity, abundances and species composition of foraminiferal assemblages of each core were assessed by non-parametric multivariate permutational analyses of variance (PERMANOVA; [108]) based on Euclidean distances and Bray–Curtis similarity. Then, for the abiotic data, a similarity profile based on permutation was tested using the SIMPROF routine to group core levels with a similar (i.e., branch with $p > 0.05$) organic matter composition. Groupings generated using the SIMPROF procedure were validated with a dissimilarity matrix based on Euclidean distance that was used in an agglomerative hierarchical clustering (routine CLUSTER). A Principal Coordinates Analysis (PCO) was also performed to describe the organic matter compounds that most accounted for variation among groups identified by the SIMPROF procedure. Finally, a non-parametric multivariate multiple regression analyses based on Bray–Curtis distances were carried out using the routine DISTLM forward [108], separately for foraminiferal abundance, assemblage composition and species richness. This latter analysis was performed to evaluate whether and how much the trophic resources (i.e., quantity and biochemical composition of the organic matter) explained dissimilarities in the composition of the foraminiferal assemblages in the four cores. The forward selection of explanatory variables was carried out under a linear regression model using 999 permutations.

3. Results

3.1. Sediment Description and Geochemistry

In the outer part of the Kveithola Trough (site 01) the sea bottom surface appeared slightly mounded with sparse IRD (Ice Rafted Debris) as evidenced in the X-ray images (Figure 2), black worm tubes, and rare shells. The sediments at the sea bottom interface (1–1.5 cm below sea floor, bsf), were clean, olive-brown (oxidized), fine-grained sand changing to soupy, bioturbated, brownish silty sand between 1.5–8 cm bsf (Figure 2). The Br/Cl content used as a proxy for marine organic matter content and related productivity [111,112] was the lowest observed in the Kveithola Trough area (Figure 2), at the same the S/Cl ratio used as a proxy of suboxic conditions [112,113]. The mean frequency curves of the studied interval present a prominent mode within the fine sand indicating shear strength conditions during deposition. The presence of sparse IRD exclude the deposition occurred through turbidity currents (i.e., [114,115]). Ref. [116] indicated the coarse-grained, condensed sequences of the outer area of the Kveithola Trough deriving from bottom current deplection of fines material operated by the warm North Atlantic Water.

In the main and minor Kveithola drifts (sites 07 and 20, respectively) the sea bottom surface was slightly hummocky with a "jelly-like" consistency at the surface with sediments pervasively bioturbated containing abundant worm tubes and a strong smell of H2S. The grain size progressively decreases inland from the main drift (site 07), to the minor drift (site 20), having bi-modal grain size spectra with main mode shifting from the coarse to the fine-graines silt. The bi-modal characteristic of the grain size spectra is an indication in support with bottom currents deposition. The Br/Cl and S/Cl ratios at both sites were distinctly higher compared to the outer shelf area (site 01). Site 22 and 23 located at a very short distance from each other on the Northern channel contained soft, soupy sediments having a jelly-like consistency.

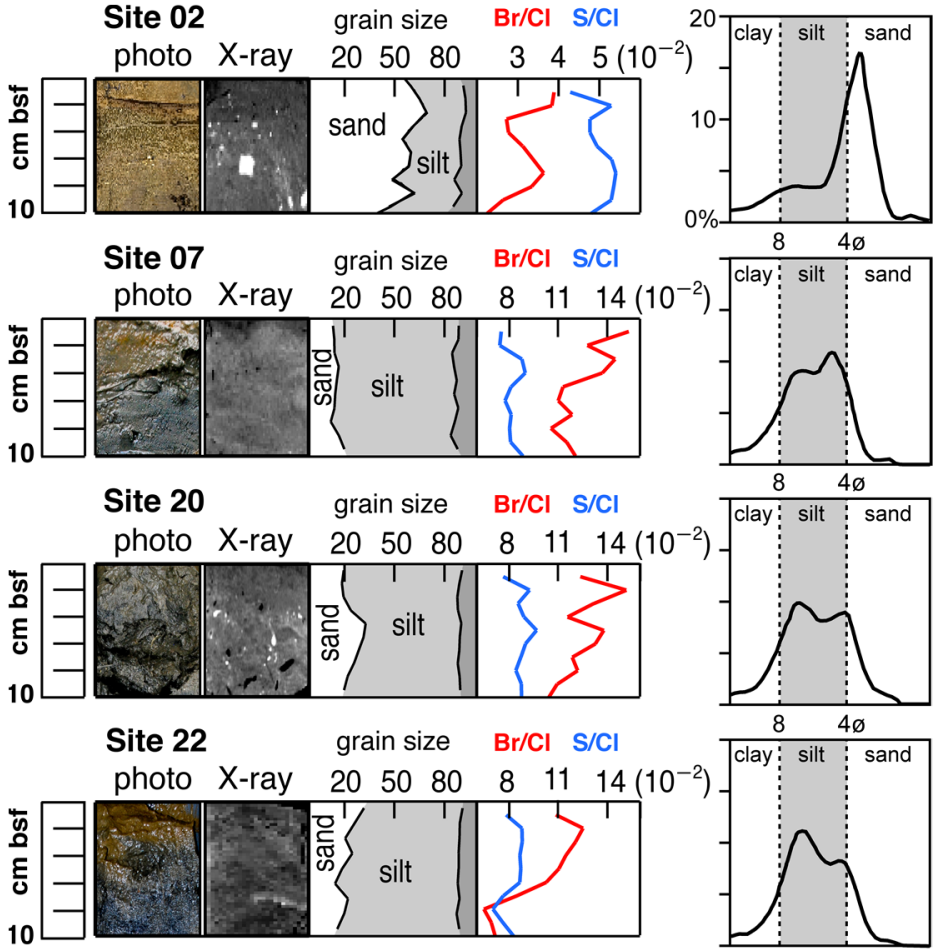

Figure 2. Sedimentological information of the studied cores including sediment photographs, X-rays (white = high density), and the down core distribution of grain size and compositional (XRF) characteristics. On the right side, we report the mean frequency curves of grain size distribution for each studied interval.

The sediments at the surface were slightly coarser-grained with respect to the middle and inner part of the trough (sites 07 and 20) but finer compared to the outer through (site 01) with sandy silt containing abundant worms and shells debris at the surface (broken shells with evidence of carbonate dissolution). The mean frequency curves apper bi-modal (Figure 2) with a principal mode within the fine silt, suggesting deposition occurred under very low-energy bottom currents. The sediments had a strong smell of H_2S with Br/Cl and S/Cl ratios considerably higher than the outer shelf but rather more similar to what was observed in the inner area of the trough (Figure 2). Therefore, in general, the sediment's grain size distribution at the sea bottom surface decreases from the outer area of the trough (site 01) towards the inner part (sites 07, 20), whereas slightly coarser sediments with respect to the inner area of the trough were observed in the Northern channel (sites 22 and 23) (Supplementary Material Table S1: Sedimentological Data).

3.2. Chemical Characterization of Sediments

Organic carbon content (Figure 3A) generally decreased slightly down-core and TOC concentrations in the drift area and in the Northern channel (sites 07, 20 and 23, average 22.4 ± 0.8, 20.6 ± 1.0, 19.8 ± 1.0 mg C g^{-1}, respectively) appeared about 2.5 times higher than in the outer shelf (site 01, average 8.5 ± 1.3 mg C g^{-1}). The significant difference among sampling sites is confirmed by the one-way ANOVA analysis ($p < 0.001$).

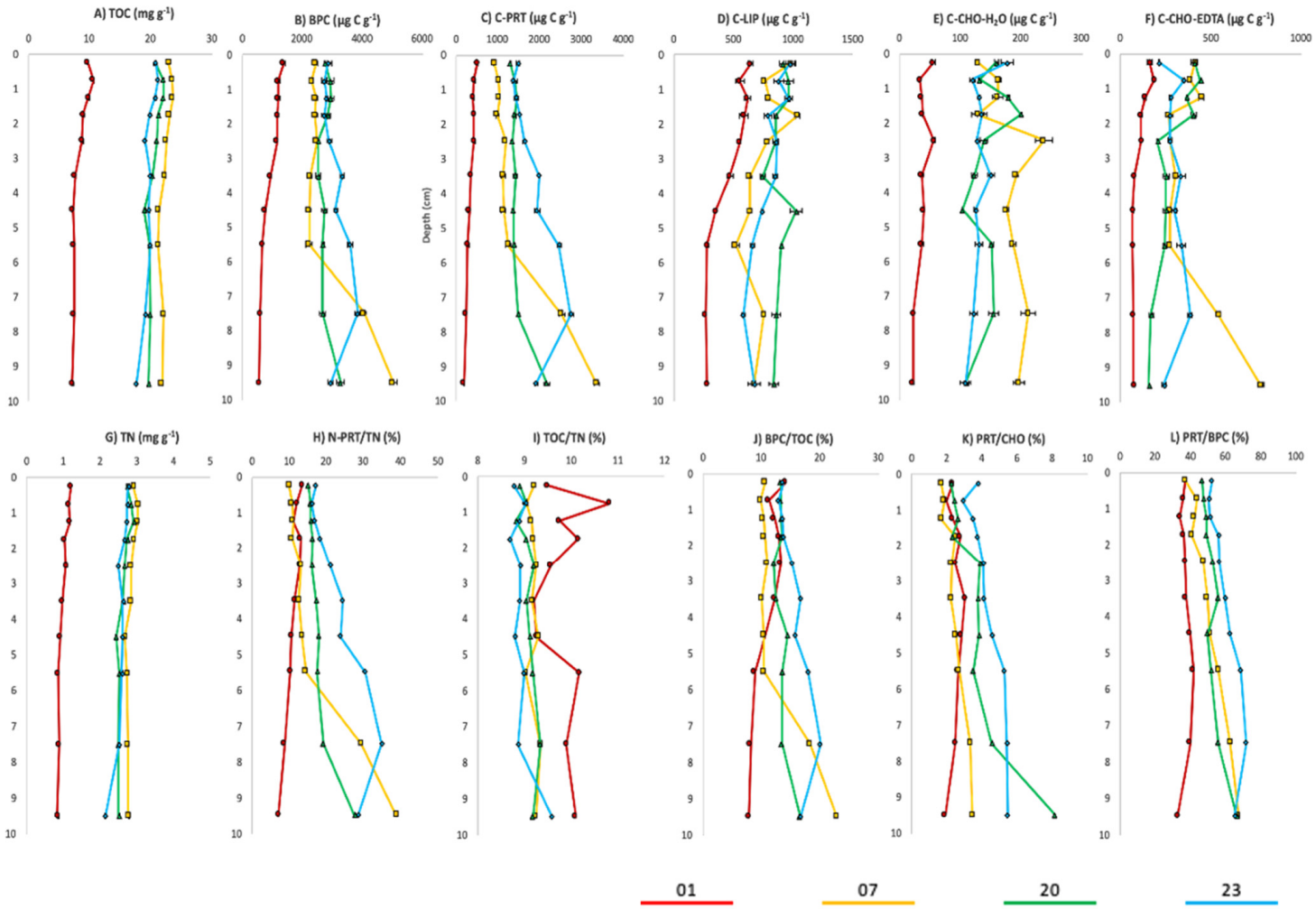

Figure 3. Chemical and biochemical elemental analyses of (**A**) Total Organic Carbon (TOC) (mg g^{-1}), (**B**) biopolymeric carbon (BPC, µg C g^{-1}), (**C**) protein (C-PRT, µg C g^{-1}), (**D**) lipid (C-LIP, µg C g^{-1}), (**E**) carbohydrate ($C\text{-}CHO_{H2O}$, µg C g^{-1}), (**F**) carbohydrate ($C\text{-}CHO_{EDTA}$, µg C g^{-1}), (**G**) Total Nitrogen (TN) (mg g^{-1}), (**H**) Protein Nitrogen/Total Nitrogen ratio (N-PRT/TN), (**I**) Organic Carbon/Total Nitrogen ratio (TOC/TN), (**J**) BPC/TOC ratio, (**K**) PRT/CHO ratio and (**L**) PRT/BPC ratio. Red line: station 01; yellow line: station 07; green line: station 20; blue line: station 22.

Similar patterns of distribution were observed for TN (Figure 3G), whose concentrations in the cores collected from inner sites (07, 20 and 23) were up to 3 times greater than those assessed in the outer shelf (site 01). TOC/TN molar ratio was generally higher and more variable down-core at site 01, where the maximum value (10.81) was noticed at the 0.5–1 cm interval. Conversely, at the other sites TOC/TN showed slight variations along sediment depth, fluctuating between 8.70 and 9.59 (average 9.37 ± 0.45) (Figure 3I). BPC concentrations were significantly lower ($p < 0.01$) in the outer shelf (average 959 ± 298 μg C g^{-1}) than in the drift area and in the Northern channel (average 2781 ± 949, 2788 ± 220, and 3073 ± 384 μg C g^{-1}, in sites 07, 20 and 23, respectively) (Figure 3B). BPC accounted for 8 to 23% of TOC concentrations in the four sites (Figure 3J). Interestingly, the main contribution of BPC to TOC was observed at the deepest layers of core at site 07 and was due to proteins. Proteins were the dominant biochemical class of BPC also at sites 07, 20 and 23 accounting for 49.8 ± 9.7, 52.3 ± 5.8, and 59.3 ± 7.4%, respectively. Concentrations, ranging from 909 to 3356 μg C g^{-1}, increased downcore. Differently, PRT represented the second dominant class, after lipids, in the core at site 01 (37.1 ± 2.7% vs. 47.7 ± 3.0%) with concentrations slightly decreasing with depth (Figure 3C). The contribution of protein nitrogen (N-PRT = 0.16 × PRT) to total nitrogen (N-PRT/TN) ranged from 7.15 to 38.9%, reaching the highest percentage at the bottom of the core at site 07 (Figure 3H). On average, in the 0–10 cm interval, N-PRT contribution increased from 11.1 ± 2.0% (site 01) to 23.1 ± 6.5% (site 23). LIP represented the other biogeochemical class of BPC at all sites (Figure 3D). On average, the highest LIP concentrations were measured along with the core at site 20 (891 ± 79 μg C g^{-1}), whereas lower values were detected along core at sites 23 (798 ± 131 μg C g^{-1}), 07 (759 ± 158 μg C g^{-1}) and 01 (461 ± 151 μg C g^{-1}). Generally, vertical LIP profiles revealed an irregular decline with sediment depth. EDTA-extractable carbohydrates displayed trends similar to proteins in cores at sites 01, 07, with the highest values observed at the bottom layers of core at site 07 (542 ± 1 and 773 ± 18 μg C g^{-1} at the 7–8 cm and 9–10 cm intervals, respectively) (Figure 3F).

Conversely, the pattern of distribution of CHO_{EDTA} in cores at sites 20 and 23 did not suggest strong relationships with the other organic matter's labile compounds. CHO_{EDTA} accounted for 5% (bottom of core at site 20) to 18% (near-surface sediments of core at site 07) of BPC. Water-soluble carbohydrates (CHO_{H2O}) displayed irregular patterns along the sediment cores, not showing any clear gradient and generally presenting low concentrations (average 38 ± 11, 178 ± 34, 145 ± 30 and 133 ± 19 μg C g^{-1}, in all sites 01, 07, 20 and 23, respectively). The lowest concentrations were measured, as for the other biochemical classes, at site 01, with values ranging from 22 to 56 μg C g^{-1} (Figure 3E). CHO_{H2O} contribution to BPC varied from 2.8 to 9.6% (average among all cores and depths: 5.1 ± 1.6%). On average, the lowest PRT:CHO ratio, equal to 1.7, was measured in the 0–1 cm interval from core at site 07, the highest, equal to 8.1, at the bottom of core at site 23 (Figure 3K).

3.3. Foraminiferal Densities and Diversity

The medium densities of live (Rose Bengal stained) foraminifera in the 0–10 cm interval (>63 μm fraction) decreased from 487 (±491) ind./10 cm^2 at 299 m water depth in site 07 main drift) to 174 (±208) ind./10 cm^2 at 334 m water depth in site 20 (minor drift) (Table 2). The Rose Bengal-stained foraminiferal abundances in the upper 1 cm layer in the >63 μm fraction followed the same trend varying from 1150 (±525) ind./10 cm^2 in site 07 to the lowest value of 542 (±35) ind./10 cm^2 in site 20 (Table 2).

Foraminifera were more abundant in the first 2 cm of both fractions >150 μm and 63–150 μm fraction, which at most stations accounted for about three-quarters of the total density (Table 2). The one-way ANOVA ($p < 0.01$) revealed significant differences in foraminiferal density between the two size fractions with a dominance of small size (63–150 μm) foraminiferal populations in all studied sites. The same analyses showed a significant variation in foraminiferal density, taxonomic composition and species richness along the three depositional settings, with values at site 01 significantly different from those observed in all other sampling sites ($p < 0.001$).

Table 2. Abundance, species richness (S), Shannon's Index (H'), Eveness (J), Average Living Depth (ALD10) calculated for the coarser, finest fraction (63–150 and >150 μm) and the entire assemblage at >63 μm. The ALD_{10} was not indicated for the total fraction >63 μm.

	Abundance (ind./10 cm^{-2})	S (n° Species)	H′	J	ALD_{10} (cm)
(0–10 cm; >150 μm)					
01	52 ± 44	56	3.17	0.78	2.93
07	91 ± 102	38	1.89	0.52	3.06
20	48 ± 62	34	1.79	0.51	2.24
22	29 ± 40	48	2.73	0.7	1.07
(0–10 cm; 63–150 μm)					
01	208 ± 300	66	3.48	0.83	1.83
07	395 ± 405	63	3.04	0.73	2.38
20	126 ± 148	55	3.16	0.79	1.64
22	252 ± 364	48	2.73	0.7	1.3
(0–10 cm; >63 μm)					
01	261 ± 342	84	3.67	0.83	
07	487 ± 491	56	2.81	0.7	
20	174 ± 208	53	2.66	0.67	
22	281 ± 402	53	3.05	0.77	

A total of 132 species were identified (0–10 cm layers, >63 μm), of which 43 were calcareous hyaline, 39 agglutinated (9 referred to the monothalamous taxa as specimens belonging to genera *Lagenammina*, *Hyperammina*, *Saccammina*, *Thurammina*, *Vanhoeffenella* grouped in the superfamily Hormosinacea) and only 8 miliolids (Figure 4, Supplementary Material Table S2: Taxonomic List). We found 41 monothalamous organic taxa, the majority of which were undescribed morphotypes and they were included in the diversity analyses because most of them belong to well-known and widely spread genera of the polar environments, as *Bowseria*, *Cylindrogullmia*, *Gloiogullmia*, and *Micrometula* (Figure 5, Supplementary Material Table S2: Taxonomic List).

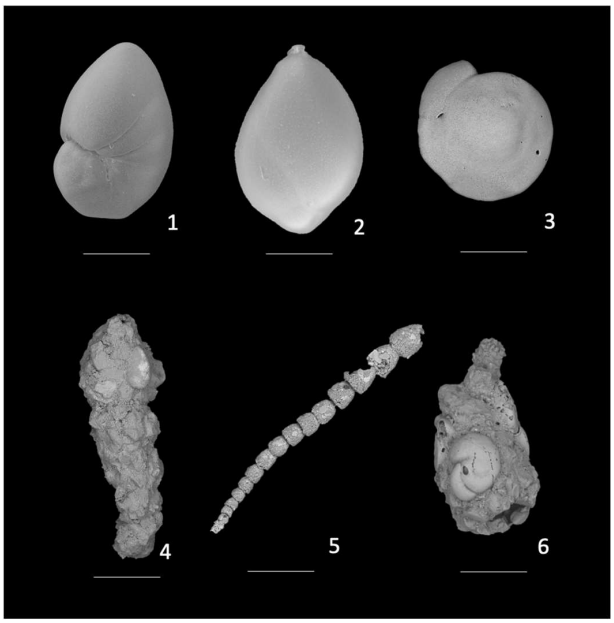

Figure 4. Scanning Electronic Microscopy (SEM) images of some of the main hard-shelled foraminiferal species. Calcareous species: 1. *Nonionellina labradorica*; 2. *Globobulimina auriculata*; 3. *Alabaminella weddellensis*; Agglutinated species: 4. *Reophax scorpiurus*; 5. *Leptohalysis scottii*; 6. *Lagenammina difflugiformis*. Scale bar 50 μm.

Figure 5. Light Microscopy (LM) images of some of the main soft-shelled monothalamous taxa RB stained. 1. *Psammophaga cristallifera*, 20× magnification; 2. *Saccaminiid* sp. 1 (silver), 20× magnification; 3. *Saccaminiid* sp. 4 (white), 20× magnification; 4. *Conqueria leavis*-like, 40× magnification; 5. *Cylindrogullmia*-like, 10× magnification; 6 *Gloiogullmia*-like, 10× magnification. Scale bar 50 µm.

Species richness (S) of the entire live benthic assemblages varied along the transect inside the Kveithola Trough from the minor drift to the grounding-zone wedge (Table 2). In site 01, a total of 84 species was recognized compared to 56 species in site 07 and 53 species in both sites 20 and 22.

The Shannon's Index value fluctuated along the transect. It was higher in site 01 ($H' = 3.67$), decreasing in site 22 ($H' = 3.05$), 07 ($H' = 2.81$) and 20 ($H' = 2.66$). The Eveness (J) showed a similar trend of species richness toward higher values at the farthest GZW (site 01; $J' = 0.83$), with medium values at the main drift (site 07; $J' = 0.70$) and Northern channel (site 22; $J' = 0.77$), and the lowest at the minor drift (site 20; $J' = 0.67$) (Table 2).

3.4. Assemblage Composition

Assemblages were dominated by polythalamous calcareous foraminifera, for the entire 0–10 cm interval, which represented between 55% (site 07 located in the main drift of the Kveithola Trough) to 64% (site 20 situated in the minor and inner drift of the Kveithola Trough) of the assemblages, whereas they did not exceed 25% of the total assemblage at 167 m water depth, in the Northern Channel of the Kveithola Trough (site 22) (Figure 6).The relative abundance of the polythalamous agglutinated was lowest (12%) at 383 m water depth in site 01 collected in the outer shelf and highest (54%) in the Northern Channel of the Kveithola Trough (site 22). Monothalamous taxa did not exceed 20% of the total assemblage in site 22 (Figure 6). Soft-shelled monothalamous taxa were not abundant in all sites, but their occurrence in the studied area represents a record of their presence in the arctic sediment. Moreover, most taxa are morphotypes underlining the importance of the description of this component among foraminifera (Figure 5). The polythalamous calcareous foraminifera dominated in all studied sites except in the finest fraction 63–150 µm of site 22 (Northern Channel) where polythalamous agglutinated foraminifera were the most representative (Figure 6). *Nonionellina labradorica* and *Adercotryma glomeratum* were dominant in the size fraction >150 µm except in the site 01 where the first centimeter of the sediment is colonized by a different and more diversified assemblage (Figure 7). In the finest fraction of all sites (63–150 µm) the phytodetritus species *Nonionella iridea* occurred instead of the species *Nonionellina labradorica* while *Adercotryma glomerata* is always present. Moreover, tiny infaunal species such as *Stainforthia* sp., *Leptohalysis scottii* occur together with the opportunistic, thin-shelled, largely epifaunal species *Alabaminella weddellensis* (Hayword et al., 2006) (Figure 4).

Monothalamous component is represented by taxa typical of polar foraminiferal assemblages [55]. We noticed the presence of *Micrometula*, *Cylindrogullmia* and *Gloiogullmia* morphotypes among allogromiids; *Saccamminid* sp. 1 (silver), *Saccamminid* sp. 2, *Saccamminid* sp. 4 (white) and *Psammophaga* morphotypes among the saccamminid component (Figure 5). They have an epifaunal and shallow infaunal microhabitat. We found two morphotypes of allogromiids with a squatter behaviour inhabiting empty tests of planktonic and benthic foraminifera respectively only at site 01.

PERMANOVA tests revealed spatial changes in composition of the foraminiferal assemblage ($p < 0.01$). The SIMPER test also revealed the presence of a large dissimilarity between depositional settings, with the largest dissimilarity observed between site 01 in the outer shelf corresponding to the grounding-zone wedges and other sites in the inner drifts of the Kveithola Trough. SIMPER showed also that the species, which mostly contribute to the observed differences, are *N. labradorica*, *A. glomeratum* and *Cylindrogullmia* sp. (Table 3).

Table 3. Dissimilarity in foraminiferal species composition among sampling periods and variables responsible for the estimated differences. Reported are the results of the SIMPER and PERMANOVA analyses (ns = not significant; * $p < 0.05$; ** $p < 0.01$; *** $p < 0.001$). In bold, species contributing to >25% of dissimilarity.

	PERMANOVA	**SIMPER**			
	P	**Dissimilarity (%)**	**Explanatory Variable (Taxon)**	**Contribution (%)**	**Cumulative (%)**
01 vs. 07	**	82.55	***Nonionellina labradorica***	**9.94**	**9.94**
			Adercotryma glomeratum	**9.71**	**19.65**
			Nonionella iridea	**5.76**	**25.42**
			Stainforthia fusiformis	5.53	30.95
			Pullenia quinqueloba	4.63	35.58
			Melonis zaandami	4.43	40.01
			Lagenammina sp. D1	3.76	43.77
			Alabaminella weddellensis	3.42	47.19
			Lagenammina difflugiformis	3.41	50.6
01 vs. 20	*	83.03	***Nonionellina labradorica***	**16.85**	**16.85**
			Trifarina angulosa	**4.98**	**21.85**
			Melonis zaandami	**4.88**	**26.74**
			Trifarina fluens	4.57	31.31
			Nonionella iridea	4.53	35.84
			Lagenammina sp. D1	4.49	40.33
			Alabaminella weddellensis	3.66	43.99
			Lagenammina difflugiformis	3.34	47.32
			Psammophaga sp. (Artic)	3.29	50.61
01 vs. 22	**	93.45	***Adercotryma glomeratum***	**9.38**	**9.384**
			***Cylindrogullmia* sp.**	**7.13**	**16.52**
			Melonis zaandami	**5.42**	**21.93**
			Trifarina fluens	**4.75**	**26.68**
			Trifarina angulosa	4.57	31.26
			Lagenammina sp. D1	4.50	35.75
			Cuneata arctica	4.20	39.95
			Nonionella iridea	3.42	43.37
			Lagenammina difflugiformis	3.37	46.75
			Islandiella helenae	3.13	49.88
			Leptohalysis scottii	2.81	52.69
07 vs. 20	ns	78.15	***Nonionellina labradorica***	**19.88**	**19.88**
			Adercotryma glomeratum	**8.47**	**28.35**
			Stainforthia fusiformis	5.47	33.83
			Nonionella iridea	5.02	38.84
			Pullenia quinqueloba	4.56	43.41
			Melonis zaandami	4.13	47.54

Table 3. *Cont.*

	PERMANOVA	SIMPER			
	P	**Dissimilarity (%)**	**Explanatory Variable (Taxon)**	**Contribution (%)**	**Cumulative (%)**
			Bolivinellina pseudopunctata	3.44	50.98
07 vs. 22	*	84.86	***Adercotryma glomeratum***	**13.07**	**13.07**
			Nonionellina labradorica	**10.23**	**23.29**
			***Cylindrogullmia* sp.**	**6.51**	**29.8**
			Stainforthia fusiformis	5.45	35.25
			Pullenia quinqueloba	4.57	39.82
			Nonionella iridea	3.96	43.78
			Bolivinellina pseudopunctata	3.77	47.55
			Melonis zaandami	3.73	51.28
20 vs. 22	*	87.89	***Nonionellina labradorica***	**16.25**	**16.25**
			Adercotryma glomeratum	**10.35**	**26.60**
			***Cylindrogullmia* sp.**	**7.37**	**33.97**
			Cuneata arctica	5.04	39.01
			Trifarina angulosa	3.65	42.66
			Trifarina fluens	3.46	46.12
			Psammophaga sp. (Artic)	3.42	49.53
			Reophax scorpiurus	3.21	52.74

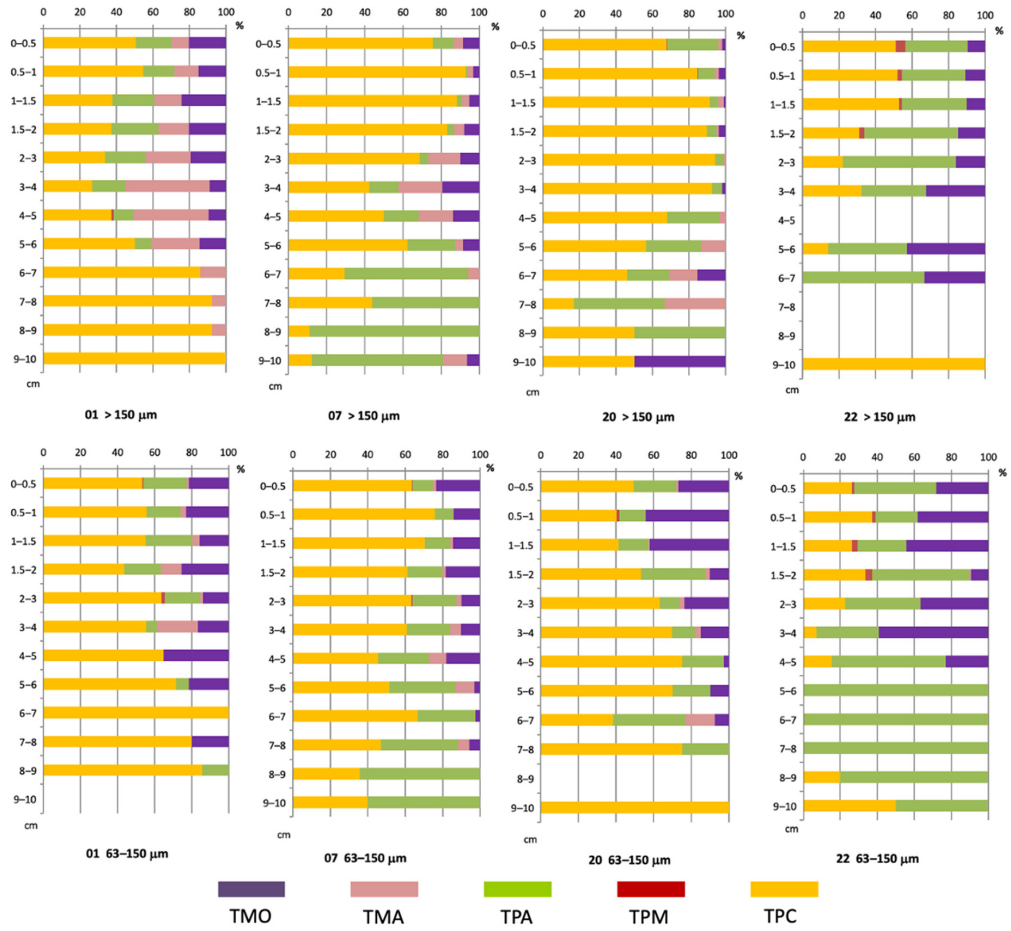

Figure 6. Relative abundance (%) of the different taxonomic components of foraminiferal assemblages in the four sampling sites. TMO = Total Monothalamous Organic; TMA = Total Monothalamous Agglutinated; TPA = Total Polythalamous Agglutinated; TPM = Total Polythalamous Miliolids; TPC = Total Polythalamous Calcareous.

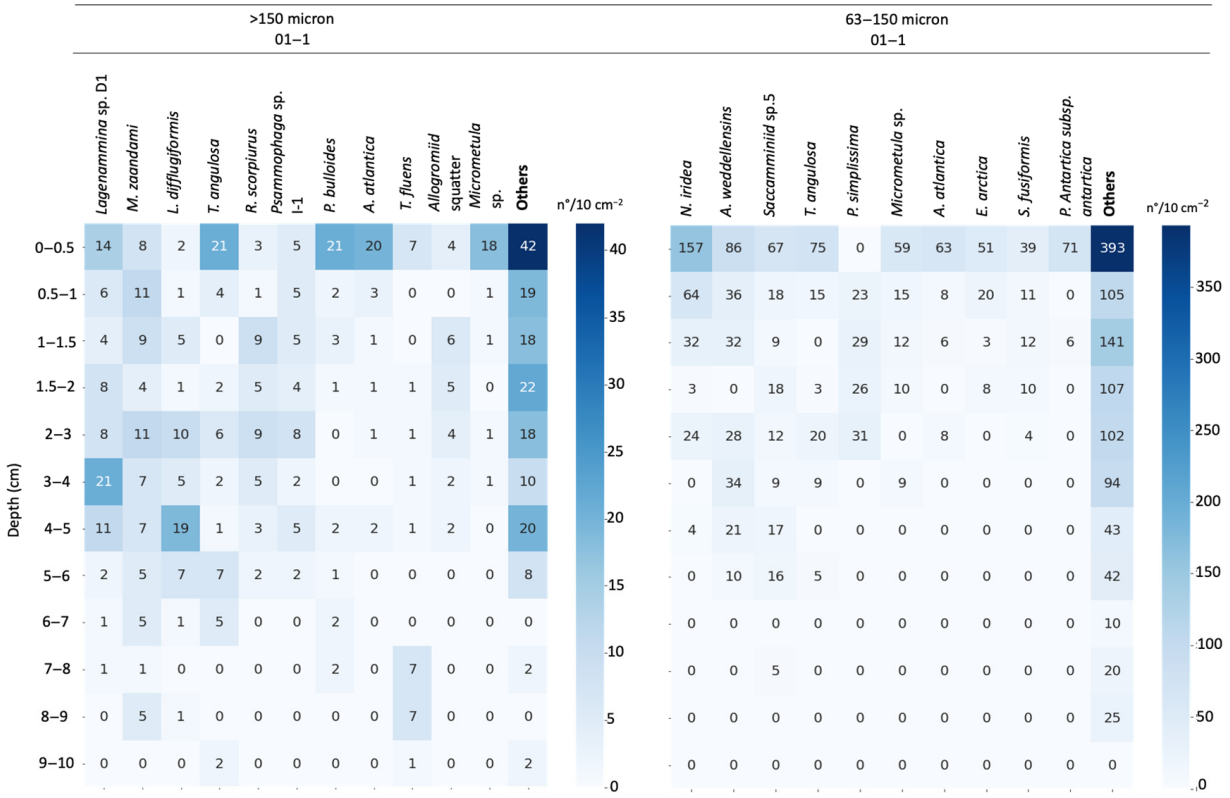

(a)

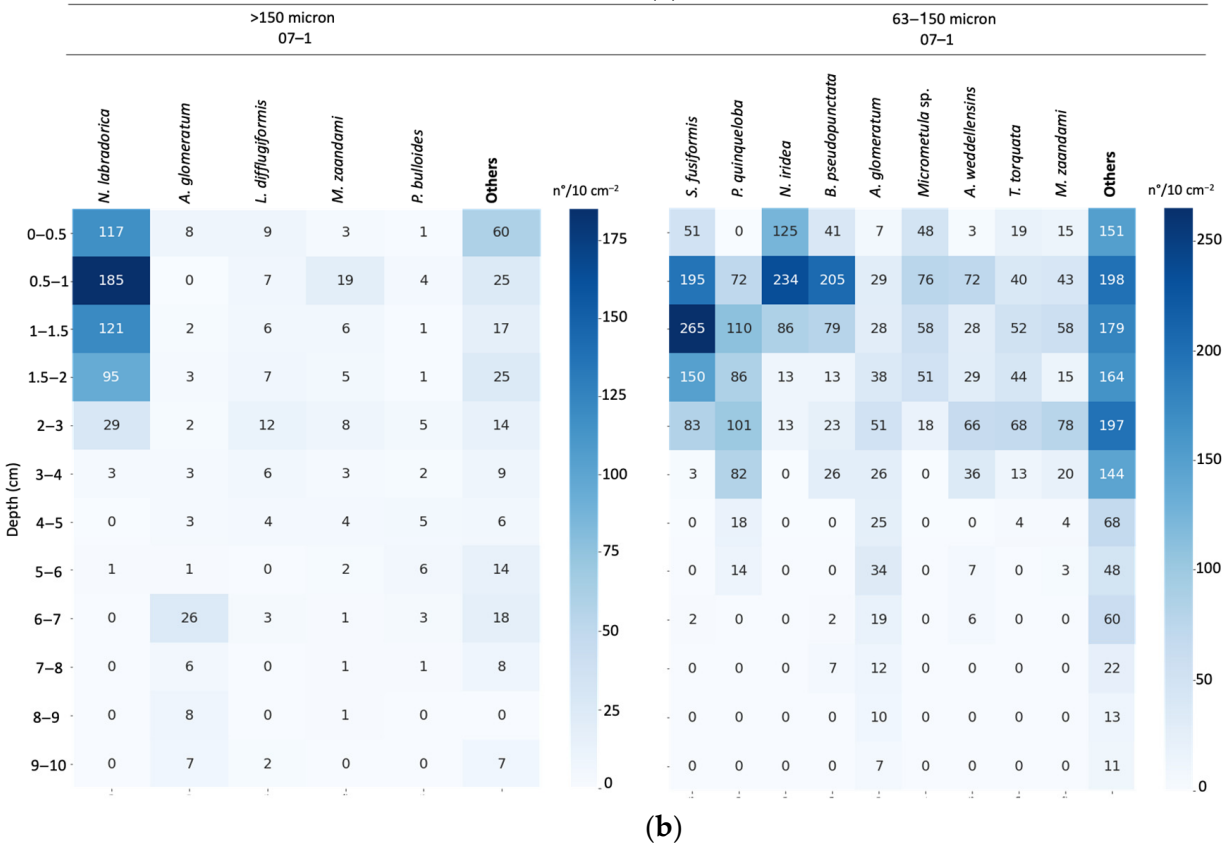

(b)

Figure 7. *Cont.*

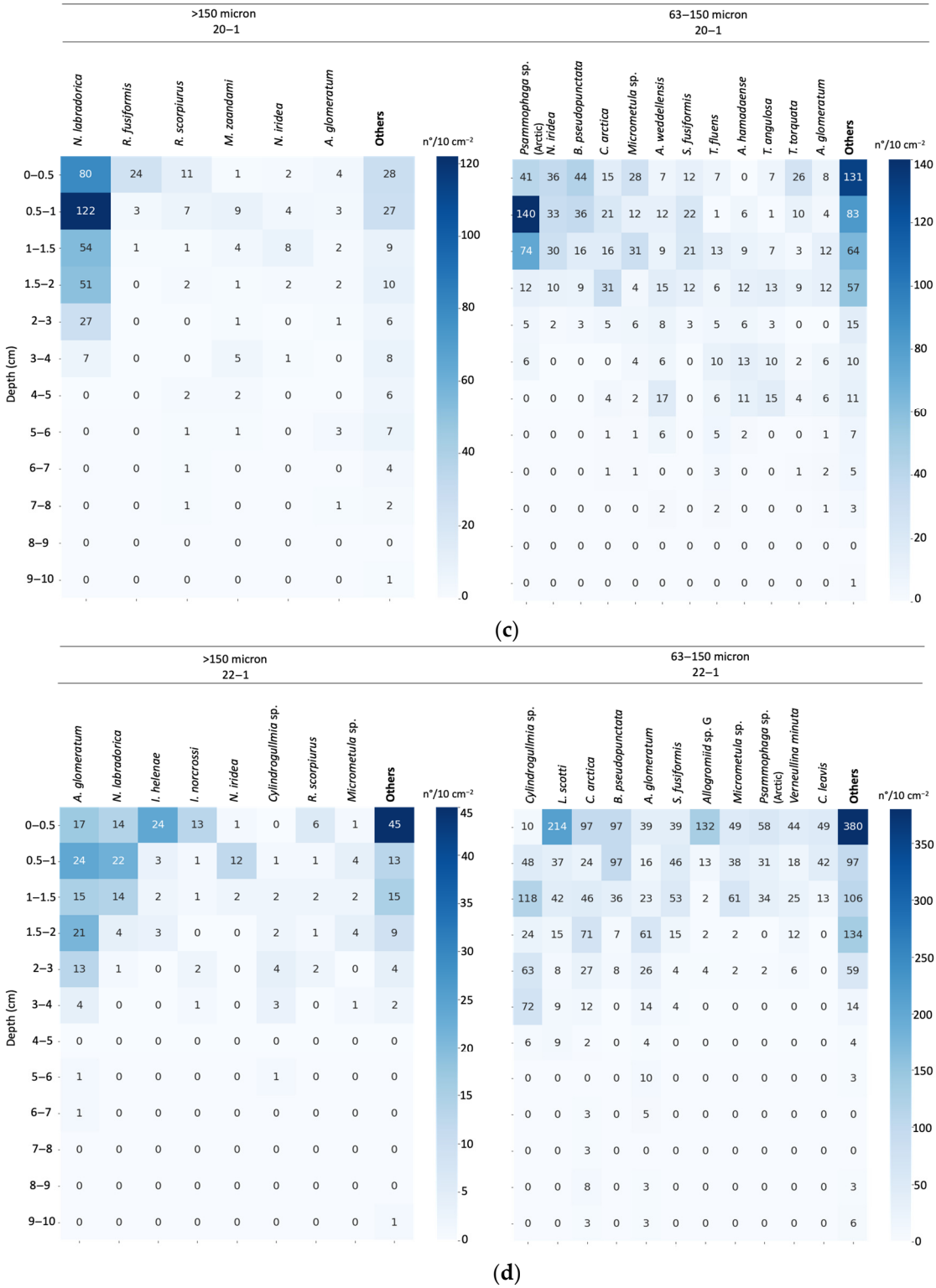

Figure 7. Vertical distribution of foraminifera for the size fraction >150 µm and 63–150 µm. Data are expressed as number of foraminifera per area (n°/10 cm^{-2}). Only species more representative are shown (>10 ind./10 cm^{-2}); "others" group includes the sum of species with the lowest density. (**a**) site 01; (**b**) site 07. Vertical distribution of foraminifera for the size fraction >150 µm and 63–150 µm. Data are expressed as number of foraminifera per area (n°/10 cm^{-2}). Only species more representative than this are shown (>10 ind./10 cm^{-2}); "others" group includes the sum of species with the lowest density. (**c**) site 20; (**d**) site 22.

3.5. Vertical Distribution of Living Foraminiferal Assemblages

Foraminiferal vertical densities were normalized for each layer to a 10 cm^2 sediment area and represented separately for the small-fraction (63–150 µm) and the >150 µm fraction considering the species with frequencies >2.5% (Figure 7). In all sites, the coarser fraction presented a foraminiferal assemblage that is strongly concentrated in the first centimeter of the sediment varying from 565 live ind./10 cm^2, at site 07, to 203 ind./10 cm^2, at site 22. For the coarser fraction of all sites, the density falls abruptly to about <50 ind./10 cm^2 starting from the 2–3 cm level excluding the site 01 where such decreasing step started at the uppermost centimeters. The foraminiferal ALD_{10} of the coarser fraction (>150 µm) varied from 1.07 to 3.06 cm at sites 22 and 07 respectively (Table 2). The assemblage from the drift (sites 07, 20 and 22) was mainly dominated by *Nonionellina labradorica* (ALD_{10} = 1.07 medium value) and *Adercotryma glomeratum* (ALD_{10} = 2.97 medium value). *Nonionellina labradorica* was always a shallow infaunal taxa and became epifaunal at site 22, while *A. glomeratum* had an infaunal (intermediate to deep) behaviour becoming epifaunal at site 22 (ALD_{10} 0.87 medium value). Monothalamous taxa as *Cylindrogullmia* sp. and squatter allogromiids, inhabiting empty benthic foraminiferal shell, had a deep infaunal position (intermediate to deep) in the sediment varying from 1.27 to 3.93 cm respectively. Site 01 showed a different species distribution along the core; *N. labradorica* and *A. glomeratum* were rare (<2.5%) and not represented in the Figure 5 and they were replaced by a different fauna from intermediate infaunal taxa (as *Alabaminella weddellensis*) to a group of epifaunal species (*Atlantinella atlantica*, *Trifarina angulosa* and *Micrometula* sp.).

The same trend was described for the small-size sediments (63–150 µm) (Figure 7). Foraminiferal assemblage was strongly concentrated in the uppermost cm (0–1 cm) of the sediment varying from 1735 live ind./10 cm^2 at site 07 to 746 ind./10 cm^2 at site 20. The ALD_{10} varied from 1.30 to 2.38 cm at sites 22 and 07, respectively and we noticed the same migration trend of infaunal species (*Stainforthia fusiformis*, *Nonionella iridea* and *Leptohalysis scottii*) towards surface sediments at site 22 from the Northern channel of the Kveithola Trough (Table 2).

3.6. Relationship between Environmental Parameters and Foraminiferal Abundance and Biodiversity

Concerning the relationships between foraminiferal assemblage and the biochemical composition of organic matter, the similarity test based on SIMPROF analyses relates the cores sampled level with similar biochemical compounds, in four distinct groups (a, b, c, d) ($p < 0.01$) confirmed via the hierarchical cluster analyses (Figure 8). Their characterization is shown in Table 4.

Table 4. Characterization of major sedimentary organic matter variables used for the hierarchical cluster analyses resulting from the SIMPROF analyses; data of foraminiferal biodiversity are included.

Variable	Simprof Group	A	B	C	D
Sedimentary Organic Matter	C-CHO-H2O (µgC/g)	37.76	204.00	165.25	141.57
	C-CHO-EDTA (µgC/g)	107.57	657.50	362.50	280.50
	C-PRT (µgC/g)	353.27	2940.50	1132.00	1630.29
	C-LIP (µgC/g)	460.56	717.00	865.50	806.44
	TOC (µgC/g)	8455.69	21,975.25	22,731.09	20,088.19
	BCP (µgC/g)	959.17	4519.27	2525.27	2858.86
	TN (µgN/g)	1002.20	2757.53	2911.28	2594.60
	N-PRT/TN	0.11	0.34	0.12	0.20
	TOC/TN	9.84	9.29	9.11	9.04
Foraminiferal Assemblage	Total species richness (S)	82	20	74	90
	N. of exclusive species	23	1	12	17
	Most caracteristics species (25% similarity within group)	*Melonis zaandami* *Lagenammina* sp. D1 *Lagenammina difflugiformis*	*Adercotryma glomeratum* *Trifarina fluens* *Reophax scorpiurus*	*Nonionellina labradorica* *Stainforthia fusiformis* *Nonionella iridea*	*Adercotryma glomeratum* *Cylindrogullmia* sp. *Cuneata arctica*

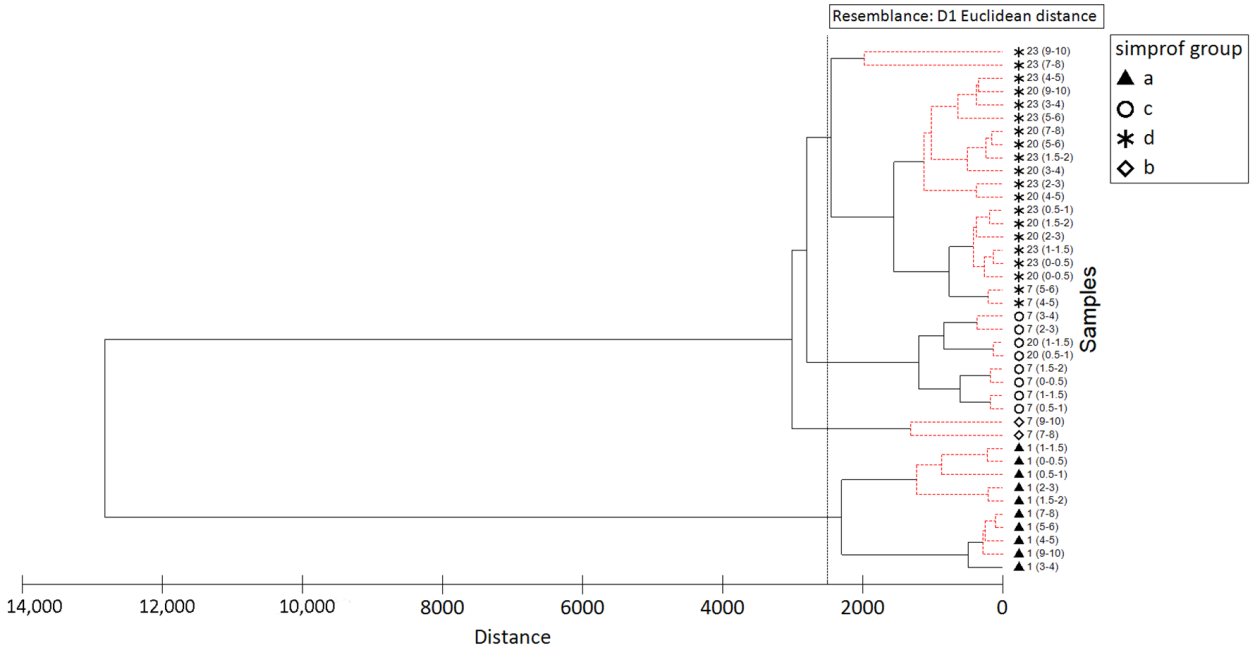

Figure 8. Hierarchical cluster analyses diagram resulting from the SIMPROF analyses of concentration of major organic components (TOC, TN, N-PRT, TOC/TN, C-PRT, C-LIP, C-CHO_{H2O}, C-CHO_{EDTA}).

The PCO1 axis (Figure 9) accounted for 98.9% of the total observed variation and clearly separated the four groups. PCO2 axis gathered 1% of the total variation. The superimposed vectors showed three sets of biochemical components of sedimentary organic matter, associated with different groups. Group-a included almost all samples (0–10 cm) of the site 01 collected at the outer shelf and it was characterized by the highest value of TOC/TN (Figures 3 and 9; Table 4). This group comprised 82 foraminiferal species, 23 of which were exclusively found in this site. The most characteristic species (species that cumulative contribute to the 25% of similarity within each group in SIMPER analyses) of this group were *Melonis zaandami*, *Lagenammina* sp. D 1 and *Lagenammina difflugiformis*.

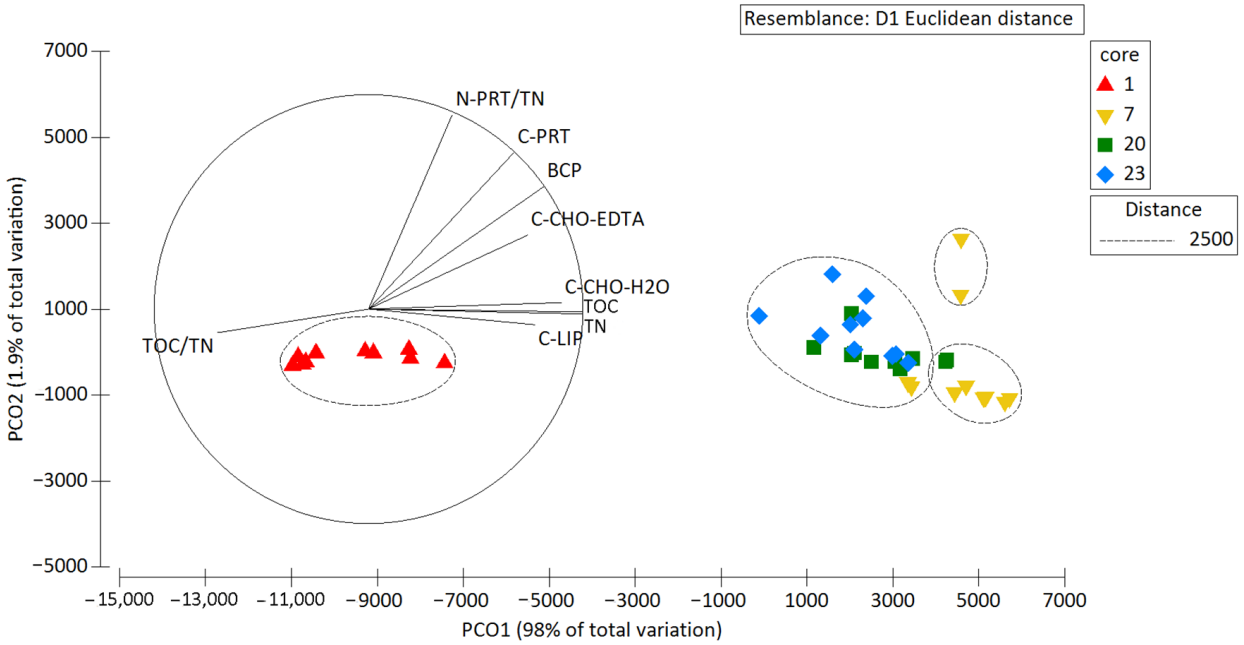

Figure 9. Principal Coordinates (PCO) analyses biplot representing the spatial distribution of core levels on the basis of concentrations of biochemical components of the sedimentary organic matter.

The group-b was represented only in thedeepest levels (7–8 and 9–10 cm) of the site 07 and it was characterized by the highest values of almost all the organic matter components, mainly BCP (Table 4) with only one exclusive species.

The group-c included the level samples of the core at site 07 from 0 to 4 cm, and the levels 0.5–1 and 1–1.5 cm of core at site 20; it is characterized by the highest values of TOC, C-LIP and TN and 74 foraminiferal species, with 12 exclusives (Figures 3 and 9; Table 4). The characteristic species of the group were *Nonionella iridea*, *Nonionellina labradorica* and *Stainforthia fusiformis*.

Finally, group-d included all the other levels of cores at site 07 and 20 and all the levels of core at site 22 (site 23 for biochemical analyses) (Figures 3 and 9; Table 4); it is characterized by the highest number of foraminiferal species, the most characteristic of which were *Adercotryma glomeratum*, *Cylindrogullmia* sp. and *Cuneata arctica*.

The multiple regression analyses (DISTLM forward) indicated that the biochemical components of sedimentary organic matter able to explain significant variations in the foraminiferal community structure were various: namely, abundance, biodiversity, and taxonomic composition (Table 5; >30% of the total variance). Indeed, changes in foraminiferal abundances depended mainly by the concentrations of N-PRT/TN BCP and C-PRT, which together explained 32% of the total variance (Table 5a). While N-PRT/TN together with C-LIP, explained changes in foraminiferal biodiversity (cumulatively 49% of variance, Table 5b). Finally, all the above mentioned biochemical organic components cumulatively explained the 45% of variance in foraminiferal species composition (Table 5c).

Table 5. Results of the DISTLM forward analyses conducted in order to evaluate the role of different sedimentary organic matter variables on (a) abundance; (b) biodiversity and (c) species composition of the foraminiferal assemblages for all the collected cores. (ns = not significant; * $p < 0.05$, ** $p < 0.01$; *** $p < 0.001$).

	Variable	F	P	Variance (%)	Variance Cumulative (%)
(a)	N-PRT/TN	5.04	***	12	12
	BCP	7.26	***	14	26
	C-PRT	3.13	***	6	32
	TN	1.68	ns	3	35
	TOC	2.38	**	4	39
	TOC/TN	2.00	**	3	43
	C-LIP	1.73	*	3	46
	C-CHO-EDTA	0.90	ns	2	47
	C-CHO-H2O	0.53	ns	1	48
(b)	N-PRT/TN	13.98	***	27	27
	C-LIP	15.72	**	22	49
	C-CHO-EDTA	2.17	ns	3	52
	C-PRT	12.65	**	13	65
	TOC/TN	2.30	ns	2	67
	C-CHO-H2O	2.00	ns	2	69
	BCP	1.73	ns	2	70
	TOC	0.81	ns	1	71
	TN	6.29	*	5	76
(c)	C-LIP	7.78	***	17	17
	C-PRT	6.64	***	13	30
	N-PRT/TN	4.97	***	9	38
	BCP	4.44	***	9	45
	TOC/TN	1.57	ns	2	48
	TOC	1.27	ns	2	49
	TN	3.37	**	5	54
	C-CHO-EDTA	0.83	ns	1	55
	C-CHO-H2O	0.65	ns	1	56

4. Discussion

4.1. Patterns of Organic Matter Quantity and Nutritional Quality

The spatial and temporal patterns of primary production, organic material export and pelagic−benthic coupling are highly variable and depth-dependent and are key drivers of benthic diversity [117–119]. Likewise, seabed sedimentary composition is perhaps the overriding driver of benthic community structure and function [120,121]. Here we discuss in detail the patterns recognized in the 4 sites investigated in the Kveithola Trough.

The four investigated sites show different pattern: in the outer shelf of the Kveithola Trough (site 01, Figure 1), organic matter values are lower than those measured in the sediments collected in the inner trough area (drift area and Northern channel) (Figure 3).

Surface sediments are characterized by silty sand and clean fine-grained sands with large scale ripple-like features, indicating the presence of strong and persistent bottom currents (Figure 2). As matter of fact, the outer part of the trough is the deepest studied area along the Kveithola Trough (400–450 m bsl) and is directly influenced by the warm and saline North Atlantic Water [122] that sweeps the outer seafloor and removes the fine sediment fraction leaving a coarse lag of sands with Ice Rafted Debris [116]. This high hydrodynamic condition obviously does not favor organic matter accumulation that instead is related to the slow settling of organic rich fine-grained sediments [123]. However, the origin of organic matter based on TOC/TN molar ratio helps discriminating marine from terrestrial organic matter in the sediments [124]. At sites located in the inner trough area, TOC/TN values, range between 8.70 and 9.59, and are uniform down-core (Figure 3F). Higher values (9.19 to 10.81) characterize the site 01 in the outer shelf. Being that TOC/TN molar ratios > 14 are representative of organic matter derived from vascular plants [125] while values between 4 and 10 relate to marine microalgae [126], it is evident that the organic matter of drift area and Northern channel is entirely marine derived. Instead, the outer shelf suggests a small continental input. This is not surprising, if we consider that the Kveithola Trough is located at the boundary of the seasonally ice-covered area of the Barents Sea. In this regard, our data agree with those reported by [127] for stations located along the Northern flank of the Kveithola Trough. Based on these data they further demonstrated that in this zone, terrestrial organic matter, deriving from the melting of sediment-bearing sea ice, represents a major component of the surface sediment organic carbon pool (0–1 cm below seafloor).

Besides, one-way ANOVA analyses, based on organic matter data, reveal a significant variation among sampling sites ($p < 0.001$). SIMPROF and PCO related analyses confirm that the TOC/TN molar ratio is a parameter responsible for the difference between the site 01 located in the outer shelf and the rest of the Kveithola sites (Figures 8 and 9).

Another interesting feature is the quality of organic matter expressed by the concentration of BPC as consumers response depends more on quality and availability than on its bulk concentration in the ecosystem [15]. Recent studies have suggested the use of carbohydrates, lipids and proteins as indicators of the trophic status of sediments in different marine ecosystems [89,92,125–128]. Specifically, biopolymeric carbon (defined as the sum of protein, lipid and carbohydrate, *sensu* [60]) is the fraction of TOC potentially available to benthic organisms [78,129] even if only 5 to 30% of these biopolymers is enzymatically digestible by consumers and, thus, readily available for heterotrophic nutrition [130].

In the outer shelf, the concentrations of BPC as well as each of its components are significantly ($p < 0.01$) lower than those measured in the drift areas (sites 7 and 20) and in Northern channel (site 23). In the latter, the enrichment in BPC concentrations and the greater content of the organic carbon, strictly of marine origin, suggest suboxic conditions at the sea bottom driven by higher oxygen demand of organisms degrading the organic matter. This condition is further confirmed by the values of Br/Cl and S/Cl ratios considerably higher than in the outer shelf.

All these data allow us to infer that at the outer site 01, oxygen consumption is limited by the lower organic matter pool and by a higher presence of refractory organic carbon, most likely due to the relatively higher contribution of terrestrial inputs. On the other

hand, the relative increase of oxygen demand in the drift area and the Northern channel may represent the limiting factor of the benthic foraminiferal community in terms of abundance and biodiversity. At the same time, however, the suboxic conditions could have contributed to preserve (in terms of quality and freshness) the BPC pool, which is only partially consumed by foraminifera.

Further elements to be considered are the protein to carbohydrate ratio (PRT: CHO) and the contribution of protein to biopolymeric carbon (PRT/BPC%). Several authors [84–89] suggest that they can be used as descriptors of both ageing and nutritional quality of the organic matter. As a matter of fact, proteins, that are degraded by bacteria more quickly than carbohydrates, are N-rich products and N is a limiting factor for benthic consumers including foraminifera. Consequently, it can be argued that a higher PRT/CHO ratio is a proxy of a fresher organic material [89].

As the PRT/CHO ratios of core samples collected from site 01 and site 07, that range between 1.9 and 3.0 and between 1.7 and 3.5 respectively, they indicate similar age and nutritional quality of the sedimentary organic matter in the two areas (Figure 3). Comparable values, ranging between 2.3 and 2.6, are also obtained in the superficial interval (0–2 cm) of the core collected at site 20. Conversely, higher values characterize the 2–10 cm interval of the core at site 20 (values between 3.9 and 8.1) and at the whole core at site 23 (values between 2.9 and 5.5), suggesting the presence of fresher organic matter in the inner trough sites and in the Northern channel.

Besides this, the quality of the organic matter in the sediments from the outer shelf is lower (lower concentrations of BPC and depletion of the PRT fraction) with respect to the sediments retrieved from the inner areas of the trough. More specifically we observe that the spatial distribution of PRT/BPC% follows an eastward gradient, increasing from the outer site 01 (PRT/BPC% = 37.1 $\pm$ 2.7%) and the main drift (site 07, PRT/BPC% = 49.8 $\pm$ 9.7%) to the minor drift (site 20, PRT/BPC% = 52.3 $\pm$ 5.8%) and Northern channel (site 22/23, PRT/BPC% = 59.3 $\pm$ 7.4%).

Therefore, the distribution of the organic matter, in term of quantity and quality, reflects this morpho-depositional subdivision and indicate that the Kveithola drift is a combination of an off-bank wedge and a confined drift [131] where the finest grain sizes and high accumulation rates occur in proximity of the moat towards the Northern flank of the trough (Figure 2). We then hypothesize a close relationship between the benthic structure and these environmental drivers as suggested for the macrofauna and foraminifera studied in the same area [16,132] that is discussed in detail in the next paragraph.

4.2. Relationships between Organic Matter Pool and Living Foraminiferal Assemblage

Previous studies [16,132] of the Kveithola area showed that the macrofaunal and foraminiferal distribution varies significantly along the main longitudinal transect of the trough despite its short length. They studied sediment cores collected in 2016 at the same position of sites analyzed in the present study, except for the new site 21. The analysis of RB-stained benthic foraminiferal assemblage showed statistically significant differences in the abundance, taxonomic composition, and vertical distribution of foraminiferal community between the outer and the inner region of the Kveithola Trough suggesting that one of the main determining factors in their spatial distribution, density, and species composition is the supply of organic matter and its quality analyzed in the first 2 cm. In particular, the outer shelf evidences a diversified benthic foraminiferal assemblage indicating an oxygenated and oligotrophic environment. The authors considered the inner part a disturbed and stressed area due to rapid organic-rich matter burial in sediments leading to oxygen-depleted environmental setting where opportunistic ant tolerant benthic species dominate. The same trend is suggested by the macrofaunal community of the Kveithola Trough characterized by the presence of opportunistic species (e.g., *Levinsenia gracilis* and *Maldane sarsi* among polychaetas, *Mendicula* cf. *pygmea* and *Yoldiella* sp. among bivalves) which are known to inhabit oxygen-depleted environments and organic-enriched sediments [132].

Our results evidence peculiar benthic foraminiferal assemblage (Figures 6 and 7) in the different areas described by the organic matter distribution in terms of quantity and quality. In particular, the foraminiferal abundance and biodiversity vary eastward along the Kveithola Trough from the outer to inner sites (01 to 20) and southward from the Northern channel to the moat in the minor drift (22 to 20).

Literature show that the distribution and abundances of the benthic foraminifera is controlled by environmental and physical variables and both organic matter in the sediment and that the dissolved oxygen concentration at the sea-floor play a primary role for the development or decline of the benthic assemblage [18,107,133,134]. Data presented in [92] further evidence the role that different components of the labile organic matter exert on benthic foraminifera. Finally, the spatial distribution of foraminifera is modelled also by the organic matter fluxes originating from seasonal phytoplankton blooms, land derived organic debris and river discharges [23,25,27,107,135–140]. In particular, in the Western Barents Sea region, the distribution of organic matter in surface sediments mainly depends on input from land-derived terrigenous and in-situ produced marine organic matter [127].

Observing in detail our results, at site 01, the terrestrial biochemical signature of organic matter, together with oxic sediment and high hydrodynamic setting coincide with a stable environment supporting an abundant and diversified foraminiferal assemblage with a well-developed infaunal behavior (Figures 3, 6 and 7; Table 2). This is possibly related to the major presence of refractory fractions of sediment organic carbon, and a consequence deeper oxygen penetration in the sediment. The occurrence of *Melonis zaandami* suggest in addition, seasonal variation of organic matter and phytodetritus pulse (Table 2; Figure 7). In fact, this species is an intermediate to deep infaunal species occurring in the Nordic Seas that shows a close correlation with the presence of altered organic matter in the sediment and is associated with more degraded food [99,141]. Furthermore, in the Nordic Seas, *M. zaandami* is also used as an indicator of high organic carbon fluxes [56,142–152].

At site 07, the benthic foraminiferal assemblage shows the highest abundances within the 0–10 cm interval (Figures 6 and 7, Table 2) with respect to the minor drift and shallower sites (20, 22). All the inner sites show a decrease of biodiversity (Table 2) with the dominance of species associated with organic-rich sediments and oxygen-depleted environments. These are the calcareous species *Nonionellina labradorica*, typical of the size fraction > 150 µm, replaced by the species *Nonionella iridea* and *Stainforthia fusiformis* in the finest fraction (63–150 µm) together with the occurrence, at both size fractions, of *Adercotryma glomeratum* (Figures 4 and 7). According to [34] that described the chloroplasts sequestration in *N. labradorica* and such behavior is thought to possibly provide oxygen to the host even in absence of it, permit to interpret the environment accordingly; furthermore *A. glomeratum* known to behave as opportunistic when there are enhanced food conditions, under either oxic or anoxic conditions [153] therefore suggesting high organic matter input.

Again, also the allogromiid genera *Micrometula* and *Cylindrogullmia*, dominating among the foraminiferal monothalamous component, and inhabiting the detritus layer of the Arctic fjords suggest anoxic condition (Figure 5) [59,101]. *Micrometula* seems dependent on fresh phytodetritus [152] while *Cylindrogullmia* lives in an extremely oxygen-deficient environment [138]. Finally, we also notice the presence of some agglutinated species as *Reophax scorpiurus* and *Lagenammina difflugiformis* considered tolerant to hypoxia [154], while *Leptohalysis scottii* as indicators of benthic eutrophication in shallow waters [92] dominates the subsurface samples in the finest fraction at the site 22.

Based on what has been said above, and on the distribution of the organic matter since the supply of rapidly digestible fraction of the organic matter controls the oxygen consumption in the sediment and the localization of the successive redox fronts, it is evident that the quantity and quality of organic matter is the main parameter controlling the foraminiferal vertical distribution in the sediment. This high concentration of metabolizable organic matter, occurring deeper in our sediment cores, especially at sites 20 and 23, could represent an excellent food source for the benthic foraminiferal consumers. However, our data suggest that the population does not benefit totally from this organic stock because,

despite the food availability, the density shows a drastic fall since the first cm in site 22. We therefore hypothesize that the relative increase of oxygen demand is the limiting factor to the benthic foraminiferal community in terms of abundance and biodiversity. Alternatively, the suboxic conditions may preserve the BPC pool, which is only partially consumed by foraminifera, reducing the percentage of organic matter that can be remineralised and hence increasing the quantity buried into the seabed. When the supply of oxygen is short, more organic material is removed from the nutrient system and left trapped in the seafloor [155]. In this regard, ref. [15] suggest that the sediment community oxygen consumption is related to BPC concentrations and the enzymatically digestible fraction of BPC varies in sediments characterized by different trophic status.

Therefore, the combination of the Kveithola benthic foraminiferal assemblage data with the PRT/CHO ratio and the contribution of protein to biopolymeric carbon (PRT/BPC%) (considered as descriptors of both ageing and nutritional quality of the organic matter, together with the quantity of BPC), evidence an inward gradient from the site 01 to the site 20 reflecting the morpho-depositional subdivision. Specifically, our data evidence an isolated area situated in proximity of the moat towards the Northern flank of the trough (site 22); we suppose that this regionalization changes depending on organic matter from subsurficial (0–2 cm) and deep (2–10 cm) sediment samples.

The statistical analyses performed on our data support all the hypotheses so far exposed, in particular:

(1) The SIMPER and ANOSIM analyses strengthen further the large variability in the foraminiferal assemblage composition among sampling sites, with the largest significant dissimilarity observed between site 01 and 7, 22 respectively (Table 3). This result, along with the variation of foraminiferal community structure at the inner drift sites, indicates that changes in the quantity and biochemical composition of sedimentary organic matter likely modulate changes in benthic foraminiferal biodiversity.

(2) The results of the multiple multivariate regression analysis also indicate that the contribution of the protein-nitrogen to TN is responsible for change in the foraminiferal assemblage and, in particular, the protein fraction of BPC explains a significant portion of the variance of either foraminiferal abundance or taxonomic composition (Table 5). These findings agree with previous statements, namely that the quantity of enzymatically digestible fraction of BPC, represented mostly by proteins, increases within the sediment and inward the Kveithola sites. On the contrary, at site 01, the benthic environment, characterized by higher refractory fractions of sediment organic carbon, may experience a deeper oxygen penetration in the sediment with respect to other Kveithola sites, thus favouring an infaunal behaviour of foraminiferal assemblage as suggested by the ALD values (Table 2).

(3) Furthermore, foraminifera are distributed in this benthic context as suggested by the hierarchical cluster analysis diagram resulting from the SIMPROF analyses (Figure 8). The group-c represents the subsuperficial samples of sites 7 and 20 (until 4 cm and 1.5 cm depth, respectively) which exclusive species are represented by some monothalamous taxa, among them several allogromiid morphotypes together with some species of agglutinated foraminifera belonging to genera *Ammodiscus*, *Glomospira* and *Trochammina*. Sites 20, 22 gather in the group-d where unique species are some opportunistic miliolids (including *Quinqueloculina seminula*) and the occurrence of *Eubuliminella exilis* known as low oxygen resistant species [154]. Conversely, group-a lumps together sediment samples of the site 01 whose exclusive species are sensible to phytodetritus input.

4.3. Relationships between High Organic Matter Accumulation in the Sediment, Foraminiferal Microhabitat and Actuopalentological Considerations

This spatial morpho-depositional subdivision also reflects the foraminiferal microhabitat, suggesting for the site 01 a trophic environment characterized by a lower percentage of labile, easily metabolizable, land-derived organic matter, except for the seasonal input of fresh phytodetritus. In these oligotrophic environmental conditions, we suppose a deeper

oxygen penetration in the sediment and a low-competition environment, justifying the low foraminiferal density (due to low food supply) and conversely a high biodiversity with the occurrence of species having a highly tolerating poor food quality (Table 2, Figure 7). Towards mesotrophic/eutrophic sites (site 7), part of the bioavailable material is introduced down-core (Table 3); the result is the creation of a favorable niche inhabited by abundant foraminifera deep in the sediment, as suggested by the total ALD_{10} (Average Living Depth) (Table 2; Figure 7). A high quantity of food availability probably does not represent a limiting factor for the benthic community at this stage, and the oxygen concentration may be high in the sediment. Finally, sites 20 and 22 draw a transversal northward transect of the Kveithola Trough characterized by eutrophic conditions (ample high percentages of BPC correlated to higher nutritional quality of the organic matter down-core for both sites) (Figure 3). This environmental setting is stressful for foraminiferal benthic community that reacts decreasing abundance and biodiversity (Table 2, Figure 7) with the occurrence of more low oxygen resistant species migrating at the sediment surface. This microhabitat difference may suggest that eutrophic (i.e., enriched in BPC concentration) sediments are characterized also by high concentrations of rapidly digestible material (sites 07, 20, 22 vs. sites 01) (Figure 9). However, increasing BPC concentrations in the sediment also may display a progressive decline of the percentage contribution of the easily metabolizable organic matter and in particular proteins. This result would imply that benthic environments are conditioned by changes in trophic status and may undergo relevant changes in the proportion of the labile and refractory fractions of sediment organic carbon. These changes could be also the result of described differences in sediment grain size and sedimentation rate, which are known to play a major role in the preservation (and, thus, lability) of the different pools of sediment organic matter [156]. Nevertheless, [15] suggest that this high accumulation of labile organic matter in the eutrophic systems could enhance the complexation of buried organic molecules with the inorganic matrix resulting in making them less available to heterotrophic nutrition [126]. In particular, proteins, as potentially labile molecules in organically enriched sediments, may be mainly buried leading to the same condition observed in the sapropel layers deposited under lacustrine conditions more than 4000 years ago [157]. The authors, using solid-state 15N nuclear magnetic resonance (NMR) demonstrated the evidence that the refractory nitrogen from an organic-rich sediment is composed primarily of amide-linked nitrogenous substances. They additionally confirmed that this amide-N derives from proteinaceous material being protected from degradation. It is probable that protection is affected by encapsulation within the macromolecular matrix forming sedimentary organic matter. Finally, [15] proposes that when BPC concentrations in the sediment exceed 2.5 mg C g^{-1}, as for our sites located in the inner drift and Northern channel, its bioavailable fraction is always less than 10%. This trophic condition, if widespread in the same area, may represent a threshold out of which accumulation of BPC leads to different organic matter bioavailability to benthic consumers. This altered condition of less available labile organic matter may happen similarly in the inner part of the drift and in particular in the proximity of the moat towards the Northern flank of the trough at the site 22.

Sapropels are also peculiar marine layers which are organic matter rich, and which occur in the Mediterranean Sea sedimentary record of the last 13.5 million years (see [158] and references therein), whose formation is commonly ascribed to deep-sea anoxia, enhanced export productivity, or a combination of these. Sapropels are a natural testbed for understanding redox condition of sea-water and carbon burial processes. However, their formation mechanisms are still debated. It is noteworthy that benthic assemblage, as foraminifera, suffer the stressed environment consequent to sapropel formation. Especially, benthic foraminifera undergo the dysoxic–anoxic conditions occurring during the sapropels deposition. As an example, in sapropel S5 deposited 124 Ky [159] the benthic assemblage is represented by specimens belonging to the genera *Bolivina*, *Stainforthia* and *Cassidulina* [160,161]. These taxa are linked to eutrophic and low oxygen environments, and they are presently abundant in the inner part of the Kveithola Trough signaling a possible organic matter burial evolution.

Therefore, the ecological study of benthic foraminifera, in this and other modern organic matter-rich sediments, will help us improve the knowledge of the meaning of the benthic assemblage that lived at the time of the fossil organic rich sediment and help us to understand the environmental condition leading to their sedimentation. This can be seen as an application of "Actuopaleontology", a discipline that [162] exists with the aim to relate biology and palaeontology, and so to better understand life on our planet.

5. Conclusions

This article provides a description of the living (stained) benthic foraminiferal assemblage of the Kveithola trough along with data of quantity and biochemical composition (in terms of, TOC, TN and biopolymeric carbon, defined as the sum of protein, lipid, and carbohydrate carbon) of the sedimentary organic matter. Spatial changes of benthic foraminiferal structure, in terms of abundance and species compositions, correspond to changes in trophic status. The result is a shift from an oligotrophic land-derived organic matter region located in the outer part of the trough to a eutrophic high metabolizable organic matter area in the inner part which comprises the drift and the Northern flank of the trough. In turn, the distribution of the organic matter and the benthic environment reflect the morpho-depositional subdivision of the Kveithola Trough and support the suggestion that the Kveithola drift represents a combination of an off-bank wedge and a confined drift where we notice the finest grain sizes and high accumulation rates in proximity of the moat towards the Northern flank of the trough.

For this reason, both the organic matter's freshness and good nutritional quality detected in the inner and the Northern flank of the trough could be the result of the better preservation of the organic matter itself, basically driven by the rapid burial of fine-grained organic-rich sediments enhanced by the cold and less saline Arctic Water flow.

Interestingly, the Kveithola benthic environment is a eutrophic hot-spot in an oligotrophic Arctic area subjected to a pulse of fresh food. This, in turn, is important because this highly dynamic depositional environment could also represent a carbon burial hot-spot sustained by hydrographic features as changes in the current strength, due to ongoing climate change from which organic matter sources on the western Barents Sea shelf could depend.

Supplementary Materials: The following supporting information can be downloaded at: https://www.mdpi.com/article/10.3390/jmse11020237/s1, Table S1: Textural and compositional (XRF) characteristics of the studied sediments; Table S2: Taxonomic List.

Author Contributions: Conceptualization, A.S. and C.M.; methodology, A.S., M.B., C.D.V. and R.G.L.; validation, A.S.; formal analysis, A.S., M.B., V.E., R.G.L. and C.M.; investigation, A.S. and M.B.; resources, C.D.V., R.G.L. and C.M.; data curation, A.S., C.D.V. and R.G.L.; writing—original draft preparation, A.S., C.M., C.D.V. and M.B.; writing—review and editing, A.S., C.M. and A.N.; visualization, A.S., F.C., V.E., R.G.L. and C.M.; supervision, A.S., A.N. and C.M. All authors have read and agreed to the published version of the manuscript.

Funding: This study was partially funded through the Italian project PNRA-CORIBAR-IT (2013/C2.01) developed in the frame of the CORIBAR international consortium including the MARUM and University of Bremen (D), OGS (IT), CSIC (ES), and GEUS (DK). Samples collection and travels were funded by the Carlsberg Foundation, sagsnummer 2012_01_0315 and the Dansk Center for Havforskning, project number 2014_04 to C.M. and A.S. The Italian PNRA supported a share the participation of the Italian team (R.G.L.) to CORIBAR cruise.

Institutional Review Board Statement: Not applicable.

Informed Consent Statement: Not applicable.

Data Availability Statement: Not applicable.

Acknowledgments: The authors acknowledge the captain, crew and scientific party of the research cruise CORIBAR (RV Maria S. Merian expedition MSM30). Special thanks go to Irene Pancotti for her collaboration in sampling and analyzing the sediment samples.

Conflicts of Interest: The authors declare no conflict of interest. The funders had no role in the design of the study; in the collection, analyses, or interpretation of data; in the writing of the manuscript; or in the decision to publish the results.

References

1. Furevik, T. Annual and Interannual Variability of Atlantic Water Temperatures in the Norwegian and Barents Seas: 1980–1996. *Deep Sea Res. Part I Oceanogr. Res. Pap.* **2001**, *48*, 383–404. [CrossRef]
2. Dalpadado, P.; Ingvaldsen, R.; Hassel, A. Zooplankton Biomass Variation in Relation to Climatic Conditions in the Barents Sea. *Polar Biol.* **2003**, *26*, 233–241. [CrossRef]
3. Sakshaug, E. Primary and Secondary Production in the Arctic Seas. In *The Organic Carbon Cycle in the Arctic Ocean*; Springer: Berlin/Heidelberg, Germany, 2004; pp. 57–81.
4. Wassmann, P.; Slagstad, D.; Riser, C.W.; Reigstad, M. Modelling the Ecosystem Dynamics of the Barents Sea including the Marginal Ice Zone: II. Carbon Flux and Interannual Variability. *J. Mar. Syst.* **2006**, *59*, 1–24. [CrossRef]
5. Barber, D.G.; Hop, H.; Mundy, C.J.; Else, B.; Dmitrenko, I.A.; Tremblay, J.-E.; Ehn, J.K.; Assmy, P.; Daase, M.; Candlish, L.M.; et al. Selected Physical, Biological and Biogeochemical Implications of a Rapidly Changing Arctic Marginal Ice Zone. *Prog. Oceanogr.* **2015**, *139*, 122–150. [CrossRef]
6. Leu, E.; Mundy, C.J.; Assmy, P.; Campbell, K.; Gabrielsen, T.M.; Gosselin, M.; Juul-Pedersen, T.; Gradinger, R. Arctic Spring Awakening—Steering Principles behind the Phenology of Vernal Ice Algal Blooms. *Prog. Oceanogr.* **2015**, *139*, 151–170. [CrossRef]
7. Michel, C.; Hamilton, J.; Hansen, E.; Barber, D.; Reigstad, M.; Iacozza, J.; Seuthe, L.; Niemi, A. Arctic Ocean Outflow Shelves in the Changing Arctic: A Review and Perspectives. *Prog. Oceanogr.* **2015**, *139*, 66–88. [CrossRef]
8. Jeffries, M.O.; Richter-Menge, J.; Overland, J.E. *Arctic Report Card 2015*; NOAA: Washington, DC, USA, 2015. Available online: http://www.arctic.noaa.gov/Report-Card (accessed on 4 December 2022).
9. Carmack, E.; Chapman, D.C. Wind-Driven Shelf/Basin Exchange on an Arctic Shelf: The Joint Roles of Ice Cover Extent and Shelf-Break Bathymetry. *Geophys. Res. Lett.* **2003**, *30*, 1778. [CrossRef]
10. Tremblay, J.-É.; Simpson, K.; Martin, J.; Miller, L.; Gratton, Y.; Barber, D.; Price, N.M. Vertical Stability and the Annual Dynamics of Nutrients and Chlorophyll Fluorescence in the Coastal, Southeast Beaufort Sea. *J. Geophys. Res. Ocean.* **2008**, *113*, C07S90. [CrossRef]
11. Stein, R.; Boucsein, B.; Meyer, H. Anoxia and High Primary Production in the Paleogene Central Arctic Ocean: First Detailed Records from Lomonosov Ridge. *Geophys. Res. Lett.* **2006**, *33*, L18606. [CrossRef]
12. Cornwell, J.C.; Conley, D.J.; Owens, M.; Stevenson, J. A Sediment Chronology of the Eutrophication of Chesapeake Bay. *Estuaries* **1996**, *19*, 488–499. [CrossRef]
13. Emeis, K.-C.; Struck, U.; Leipe, T.; Pollehne, F.; Kunzendorf, H.; Christiansen, C. Changes in the C, N, P Burial Rates in Some Baltic Sea Sediments over the Last 150 Years—Relevance to P Regeneration Rates and the Phosphorus Cycle. *Mar. Geol.* **2000**, *167*, 43–59. [CrossRef]
14. Farías, L. Remineralization and Accumulation of Organic Carbon and Nitrogen in Marine Sediments of Eutrophic Bays: The Case of the Bay of Concepcion, Chile. *Estuar. Coast. Shelf Sci.* **2003**, *57*, 829–841. [CrossRef]
15. Pusceddu, A.; Dell'Anno, A.; Fabiano, M.; Danovaro, R. Quantity and Bioavailability of Sediment Organic Matter as Signatures of Benthic Trophic Status. *Mar. Ecol. Prog. Ser.* **2009**, *375*, 41–52. [CrossRef]
16. Caridi, F.; Sabbatini, A.; Bensi, M.; Kovačević, V.; Lucchi, R.G.; Morigi, C.; Povea, P.; Negri, A. Benthic Foraminiferal Assemblages and Environmental Drivers along the Kveithola Trough (NW Barents Sea). *J. Mar. Syst.* **2021**, *224*, 103616. [CrossRef]
17. Murray, J.W. *Ecology and Applications of Benthic Foraminifera*; Cambridge University Press: Cambridge, UK, 2006; p. 426.
18. Louvari, M.A.; Drinia, H.; Kontakiotis, G.; Di Bella, L.; Antonarakou, A.; Anastasakis, G. Impact of Latest-Glacial to Holocene Sea-Level Oscillations on Central Aegean Shelf Ecosystems: A Benthic Foraminiferal Palaeoenvironmental Assessment of South Evoikos Gulf, Greece. *J. Mar. Syst.* **2019**, *199*, 103181. [CrossRef]
19. Murray, J.W.; Alve, E. Benthic Foraminifera as Indicators of Environmental Change: Estuaries, Shelf and Upper Slope. In *Environmental Quaternary Micropalaeontology*; Haslett, S.R., Ed.; Hodder Arnold: London, UK, 2002; pp. 59–90.
20. Nigam, R.; Saraswat, R.; Panchang, R. Application of Foraminifers in Ecotoxicology: Retrospect, Perspect and Prospect. *Environ. Int.* **2006**, *32*, 273–283. [CrossRef]
21. Frontalini, F.; Coccioni, R. Benthic Foraminifera as Bioindicators of Pollution: A Review of Italian Research over the Last Three Decades. *Rev. De Micropaléontologie* **2011**, *54*, 115–127. [CrossRef]
22. Fossile, E.; Sabbatini, A.; Spagnoli, F.; Caridi, F.; Dell'Anno, A.; De Marco, R.; Dinelli, E.; Droghini, E.; Tramontana, M.; Negri, A. Sensitivity of Foraminiferal-Based Indices to Evaluate the Ecological Quality Status of Marine Coastal Benthic Systems: A Case Study of the Gulf of Manfredonia (Southern Adriatic Sea). *Mar. Pollut. Bull.* **2021**, *163*, 111933. [CrossRef]
23. Jorissen, F.J.; Barmawidjaja, D.M.; Puskaric, S.; Van der Zwaan, G.J. Vertical Distribution of Benthic Foraminifera in the Northern Adriatic Sea: The Relation with the Organic Flux. *Mar. Micropaleontol.* **1992**, *19*, 131–146. [CrossRef]
24. Moodley, L.; Boschker, H.T.S.; Middelburg, J.J.; Pel, R.; Herman, P.M.J.; De Deckere, E.; Heip, C.H.R. Ecological Significance of Benthic Foraminifera: 13C Labelling Experiments. *Mar. Ecol. Prog. Ser.* **2000**, *202*, 289–295. [CrossRef]
25. Barmawidjaja, D.M.; Van der Zwaan, G.J.; Jorissen, F.J.; Puskaric, S. 150 Years of Eutrophication in the Northern Adriatic Sea: Evidence from a Benthic Foraminiferal Record. *Mar. Geol.* **1995**, *122*, 367–384. [CrossRef]

26. Loubere, P.; Fariduddin, M. Benthic Foraminifera and the Flux of Organic Carbon to the Seabed. *Mod. Foraminifer.* **1999**, 181–199.
27. Gooday, A.J. Deep-Sea Benthic Foraminiferal Species Which Exploit Phytodetritus: Characteristic Features and Controls on Distribution. *Mar. Micropaleontol.* **1993**, *22*, 187–205. [CrossRef]
28. Altenbach, A.V.; Pflaumann, U.; Schiebel, R.; Thies, A.; Timm, S.; Trauth, M. Scaling Percentages and Distributional Patterns of Benthic Foraminifera with Flux Rates of Organic Carbon. *J. Foraminifer. Res.* **1999**, *29*, 173–185.
29. Graf: Benthic-Pelagic Coupling: A Benthic View—Google Scholar. Available online: https://scholar.google.com/scholar_lookup?title=Benthic-pelagic%20coupling%3A%20a%20benthic%20view&publication_year=1992&author=G.%20Graf (accessed on 30 November 2022).
30. Goedkoop, W.; Gullberg, K.R.; Johnson, R.K.; Ahlgren, I. Microbial Response of a Freshwater Benthic Community to a Simulated Diatom Sedimentation Event: Interactive Effects of Benthic Fauna. *Microb. Ecol.* **1997**, *34*, 131–143. [CrossRef]
31. Middelburg, J.J.; Barranguet, C.; Boschker, H.T.; Herman, P.M.; Moens, T.; Heip, C.H. The Fate of Intertidal Microphytobenthos Carbon: An in Situ 13C-Labeling Study. *Limnol. Oceanogr.* **2000**, *45*, 1224–1234. [CrossRef]
32. Mackensen, A.; Douglas, R.G. Down-Core Distribution of Live and Dead Deep-Water Benthic Foraminifera in Box Cores from the Weddell Sea and the California Continental Borderland. *Deep Sea Res. Part A Oceanogr. Res. Pap.* **1989**, *36*, 879–900. [CrossRef]
33. Gooday, A.J.; Bernhard, J.M.; Levin, L.A.; Suhr, S.B. Foraminifera in the Arabian Sea Oxygen Minimum Zone and Other Oxygen-deficient Settings: Taxonomic Composition, Diversity, and Relation to Metazoan Faunas. *Deep. Sea Res. Part II Top. Stud. Oceanogr.* **2000**, *47*, 25–54. [CrossRef]
34. Bernhard, J.M.; Sen Gupta, B.K. Foraminifera of Oxygen-Depleted Environments. In *Modern Foraminifera*; Springer: Berlin/Heidelberg, Germany, 1999; pp. 201–216.
35. Mallon, J.; Glock, N.; Schönfeld, J. The Response of Benthic Foraminifera to Low-Oxygen Conditions of the Peruvian Oxygen Minimum Zone. In *Anoxia*; Springer: Berlin/Heidelberg, Germany, 2012; pp. 305–321.
36. Sergeeva, N.G.; Gooday, A.J.; Mazlumyan, S.A.; Kolesnikova, E.A.; Lichtschlag, A.; Kosheleva, T.N.; Anikeeva, O.V. Meiobenthos of the Oxic/Anoxic Interface in the Southwestern Region of the Black Sea: Abundance and Taxonomic Composition. In *Anoxia*; Springer: Berlin/Heidelberg, Germany, 2012; pp. 369–401.
37. Corliss, B.H. Microhabitats of Benthic Foraminifera within Deep-Sea Sediments. *Nature* **1985**, *314*, 435–438. [CrossRef]
38. Corliss, B.H.; Emerson, S. Distribution of Rose Bengal Stained Deep-Sea Benthic Foraminifera from the Nova Scotian Continental Margin and Gulf of Maine. *Deep Sea Res. Part A. Oceanogr. Res. Pap.* **1990**, *37*, 381–400. [CrossRef]
39. Risgaard-Petersen, N.; Langezaal, A.M.; Ingvardsen, S.; Schmid, M.C.; Jetten, M.S.; Op den Camp, H.J.; Derksen, J.W.; Pina-Ochoa, E.; Eriksson, S.P.; Peter Nielsen, L. Evidence for Complete Denitrification in a Benthic Foraminifer. *Nature* **2006**, *443*, 93–96. [CrossRef] [PubMed]
40. Pina-Ochoa, E.; Alvarez-Cobelas, M. Seasonal Nitrogen Dynamics in a Seepage Lake Receiving High Nitrogen Loads. *Mar. Freshw. Res.* **2009**, *60*, 435–445. [CrossRef]
41. Koho, K.A.; Piña-Ochoa, E. Benthic Foraminifera: Inhabitants of Low-Oxygen Environments. In *Anoxia*; Cellular Origin, Life in Extreme Habitats and Astrobiology; Altenbach, A.V., Bernhard, J.M., Seckbach, J., Eds.; Springer: Dordrecht, The Netherlands, 2012; Volume 21, pp. 249–285. ISBN 978-94-007-1895-1.
42. Korsun, S.A.; Pogodina, I.A.; Tarasov, G.A.; Matishov, G.G. Foraminifera of the Barents Sea: Hydrobiology and Quaternary Paleoecology. *Kola Sci. Cent. Publ. Russ. Acad. Sci. Apatity* **1994**, 140. Available online: https://scholar.google.com/scholar?hl=it&as_sdt=0,5&cluster=1408039786455229986 (accessed on 4 December 2022).
43. Ivanova, E.V.; Ovsepyan, E.A.; Risebrobakken, B.; Vetrov, A.A. Downcore Distribution of Living Calcareous Foraminifera and Stable Isotopes in the Western Barents Sea. *J. Foraminifer. Res.* **2008**, *38*, 337–356. [CrossRef]
44. Saher, M.H.; Kristensen, D.K.; Hald, M.; Korsun, S.; Jørgensen, L.L. Benthic Foraminifera Assemblages in the Central Barents Sea: An Evaluation of Combining Live and Total Fauna Studies in Tracking Environmental Change. *Nor. J. Geol. /Nor. Geol. Foren.* **2009**, *89*, 149–161.
45. Dijkstra, N. *Benthic Foraminifera as Indicators of Natural Variability and Anthropogenic Impact*; University of Tromsø: Tromsø, Norway, 2013.
46. Carbonara, K.; Mezgec, K.; Varagona, G.; Musco, M.E.; Lucchi, R.G.; Villa, G.; Morigi, C.; Melis, R.; Caffau, M. Palaeoclimatic Changes in Kveithola, Svalbard, during the Late Pleistocene Deglaciation and Holocene: Evidences from Microfossil and Sedimentary Records. *Palaeogeogr. Palaeoclimatol. Palaeoecol.* **2016**, *463*, 136–149. [CrossRef]
47. Ivanova, E.; Murdmaa, I.; de Vernal, A.; Risebrobakken, B.; Peyve, A.; Brice, C.; Seitkalieva, E.; Pisarev, S. Postglacial Paleoceanography and Paleoenvironments in the Northwestern Barents Sea. *Quat. Res.* **2019**, *92*, 430–449. [CrossRef]
48. Gamboa-Sojo, V.M.; Husum, K.; Caridi, F.; Lucchi, R.G.; Bensi, M.; Kovačević, V.; Sabbatini, A.; Langone, L.; Dominiczak, A.T.; Povea, P.; et al. Living and Dead Foraminiferal Assemblages of the Last Decades from Kveithola Trough: Taphonomic Processes and Ecological Highlights. *Mar. Micropaleontol.* **2021**, *166*, 102014. [CrossRef]
49. Steinsund, P.I.; Hald, M. Recent Calcium Carbonate Dissolution in the Barents Sea: Paleoceanographic Applications. *Mar. Geol.* **1994**, *117*, 303–316. [CrossRef]
50. Hald, M.; Steinsund, P.I. Benthic Foraminifera and Carbonate Dissolution in the Surface Sediments of the Barents and Kara Seas. *Ber. Zur Polarforsch.* **1996**, *212*, 285–307.
51. Basov, V.A.; Slobodin, V.Y. Complexes of Recent and Late Cenozoic Foraminifera of WeStern Soviet Arctic. The Antropogene Period of the Arctic and Subarctic. *Tr. Nauchn. Issled. Inst. Geol. Arkt. Gosud. Geol. Kom. SSSR* **1965**, *143*, 190–210.

52. Digas, L.A. Distribution of Foraminifers in Surface Sediments of the Barents Sea and Adjacent Parts of the Norwegian-Greenland Basin. PhD Thesis, Saratov State University, Saratov, Russia, 1969; 27p. (In Russian).
53. Digas, L.A. A Zoogeographic Zonation of the Barents Sea Based on Foraminifera. *Geol. Issues South Ural. Volga [Vopr. Geol. Yuzhnogo Ural. I Povolzhja]. Saratov Saratov State Univ. Publ* **1970**, 127–142. Available online: https://scholar.google.com/scholar?hl=it&as_sdt=0%2C5&q=Digas%2C+1970&btnG= (accessed on 4 December 2022).
54. Østby, K.L.; Nagy, J. Foraminiferal Distribution in the Western Barents Sea, Recent and Quaternary. *Polar Res.* **1982**, *1982*, 53–87. [CrossRef]
55. Polyak, L.V. *Foraminifers of Bottom Sediments of the Barents and Kara Sea and Their Stratigraphic Significance*; Abstract of Kandidat Disseration; LGI: Leningrad, Russia, 1985.
56. Hald, M.; Steinsund, P.I. Distribution of Surface Sediment Benthic Foraminifera in the Southwestern Barents Sea. *J. Foraminifer. Res.* **1992**, *22*, 347–362. [CrossRef]
57. Kucharska, M.; Kujawa, A.; Pawłowska, J.; Łącka, M.; Szymańska, N.; Lønne, O.J.; Zajączkowski, M. Seasonal Changes in Foraminiferal Assemblages along Environmental Gradients in Adventfjorden (West Spitsbergen). *Polar Biol.* **2019**, *42*, 569–580. [CrossRef]
58. Fossile, E.; Nardelli, M.P.; Jouini, A.; Lansard, B.; Pusceddu, A.; Moccia, D.; Michel, E.; Péron, O.; Howa, H.; Mojtahid, M. Benthic Foraminifera as Tracers of Brine Production in the Storfjorden "Sea Ice Factory". *Biogeosciences* **2020**, *17*, 1933–1953. [CrossRef]
59. Sabbatini, A.; Morigi, C.; Negri, A.; Gooday, A.J. Distribution and Biodiversity of Stained Monothalamous Foraminifera from Tempelfjord, Svalbard. *J. Foraminifer. Res.* **2007**, *37*, 93–106. [CrossRef]
60. Fichez, R. Composition and Fate of Organic-Matter in Submarine Cave Sediments-Implications for the Biogeochemical Cycle of Organic-Carbon. *Oceanol. Acta* **1991**, *14*, 369–377.
61. Rebesco, M.; Liu, Y.; Camerlenghi, A.; Winsborrow, M.; Laberg, J.S.; Caburlotto, A.; Diviacco, P.; Accettella, D.; Sauli, C.; Wardell, N.; et al. Deglaciation of the Western Margin of the Barents Sea Ice Sheet—A Swath Bathymetric and Sub-Bottom Seismic Study from the Kveithola Trough. *Mar. Geol.* **2011**, *279*, 141–147. [CrossRef]
62. Rüther, D.C.; Bjarnadóttir, L.R.; Junttila, J.; Husum, K.; Rasmussen, T.L.; Lucchi, R.G.; Andreassen, K. Pattern and Timing of the Northwestern Barents Sea Ice Sheet Deglaciation and Indications of Episodic Holocene Deposition: Barents Sea Ice Sheet Deglaciation and Episodic Holocene Deposition. *Boreas* **2012**, *41*, 494–512. [CrossRef]
63. Bjarnadóttir, L.R.; Rüther, D.C.; Winsborrow, M.C.M.; Andreassen, K. Grounding-Line Dynamics during the Last Deglaciation of Kveithola, W Barents Sea, as Revealed by Seabed Geomorphology and Shallow Seismic Stratigraphy: Grounding Line Dynamics, W Barents Sea. *Boreas* **2013**, *42*, 84–107. [CrossRef]
64. Ottesen, D.; Dowdeswell, J.A. Assemblages of Submarine Landforms Produced by Tidewater Glaciers in Svalbard. *J. Geophys. Res. Earth Surf.* **2006**, *111*, F01016. [CrossRef]
65. Dowdeswell, J.A.; Ottesen, D.; Evans, J.; Cofaigh, C.; Anderson, J.B. Submarine Glacial Landforms and Rates of Ice-Stream Collapse. *Geology* **2008**, *36*, 819–822. [CrossRef]
66. Rebesco, M.; Özmaral, A.; Urgeles, R.; Accettella, D.; Lucchi, R.G.; Rüther, D.; Winsborrow, M.; Llopart, J.; Caburlotto, A.; Lantzsch, H.; et al. Evolution of a High-Latitude Sediment Drift inside a Glacially-Carved Trough Based on High-Resolution Seismic Stratigraphy (Kveithola, NW Barents Sea). *Quat. Sci. Rev.* **2016**, *147*, 178–193. [CrossRef]
67. Lucchi, R.G.; Kovacevic, V.; De Vittor, C.; Bazzaro, M.; Bensi, M.; De Ponte, D.; Laterza, R.; Musco, M.E.; Relitti, F.; Rui, L. Burster: Bottom Currents in a Stagnant Environment; 2016. Available online: https://scholar.google.com/scholar?hl=it&as_sdt=0%2C5&q=+Lucchi%2C+R.G.%3B+Kovacevic%2C+V.%3B+De+Vittor%2C+C.%3B+Bazzaro%2C+M.%3B+Bensi%2C+M.%3B+De+Ponte%2C+D.%3B+Laterza%2C+R.%3B+Musco%2C+M.E.%3B+Relitti%2C+F.%3B+Rui%2C+L.+Bur-ster%3A+Bottom+Currents+in+a+Stagnant+Environment%3B+2016&btnG= (accessed on 4 December 2022).
68. Hanebuth, T.J.; Lantzsch, H.; Bergenthal, M.; Caburlotto, A.; Dippold, S.; Düßmann, R.; Freudenthal, T.; Hörner, T.; Kaszemeik, K.; Klar, S. CORIBAR-Ice Dynamics and Meltwater Deposits: Coring in the Kveithola Trough, NW Barents Sea. Cruise MSM30. 16 July–15 August 2013, Tromsø (Norway)-Tromsø (Norway). *Ber. MARUM-Zent. Für Mar. Umweltwiss. Fachbereich Geowiss. Univ. Brem.* **2013**, *299*. Available online: https://publications.marum.de/2347/ (accessed on 4 December 2022).
69. Loeng, H. Features of the Physical Oceanographic Conditions of the Barents Sea. *Polar Res.* **1991**, *10*, 5–18. [CrossRef]
70. Piepenburg, D.; Schmid, M.K. Brittle Star Fauna (Echinodermata: Ophiuroidea) of the Arctic Northwestern Barents Sea: Composition, Abundance, Biomass and Spatial Distribution. *Polar Biol.* **1996**, *16*, 383–392. [CrossRef]
71. Piepenburg, D.; Schmid, M.K. A Photographic Survey of the Epibenthic Megafauna of the Arctic Laptev Sea Shelf: Distribution, Abundance, and Estimates of Biomass and Organic Carbon Demand. *Mar. Ecol. Prog. Ser.* **1997**, *147*, 63–75. [CrossRef]
72. Grebmeier, J.M.; Cooper, L.W.; Feder, H.M.; Sirenko, B.I. Ecosystem Dynamics of the Pacific-Influenced Northern Bering and Chukchi Seas in the Amerasian Arctic. *Prog. Oceanogr.* **2006**, *71*, 331–361. [CrossRef]
73. Pella, E.; Colombo, B. Study of Carbon, Hydrogen and Nitrogen Determination by Combustion-Gas Chromatography. *Microchim. Acta* **1973**, *61*, 697–719. [CrossRef]
74. Nieuwenhuize, J.; Maas, Y.E.; Middelburg, J.J. Rapid Analysis of Organic Carbon and Nitrogen in Particulate Materials. *Mar. Chem.* **1994**, *45*, 217–224. [CrossRef]
75. Blasutto, O.; Cibic, T.; Vittor, C.D.; Umani, S.F. Microphytobenthic Primary Production and Sedimentary Carbohydrates along Salinity Gradients in the Lagoons of Grado and Marano (Northern Adriatic Sea). *Hydrobiologia* **2005**, *550*, 47–55. [CrossRef]

76. Dubois, M.; Gilles, K.A.; Hamilton, J.K.; Rebers, P.T.; Smith, F. Colorimetric Method for Determination of Sugars and Related Substances. *Anal. Chem.* **1956**, *28*, 350–356. [CrossRef]
77. Gerchakov, S.M.; Hatcher, P.G. Improved Technique for Analysis of Carbohydrates in Sediments 1. *Limnol. Oceanogr.* **1972**, *17*, 938–943. [CrossRef]
78. Fabiano, M.; Danovaro, R.; Fraschetti, S. A Three-Year Time Series of Elemental and Biochemical Composition of Organic Matter in Subtidal Sandy Sediments of the Ligurian Sea (Northwestern Mediterranean). *Cont. Shelf Res.* **1995**, *15*, 1453–1469. [CrossRef]
79. Hartree, E.F. Determination of Protein: A Modification of the Lowry Method That Gives a Linear Photometric Response. *Anal. Biochem.* **1972**, *48*, 422–427. [CrossRef]
80. Rice, D.L. The Detritus Nitrogen Problem: New Observations and Perspectives from Organic Geochemistry. *Mar. Ecol. Prog. Ser.* **1982**, *9*, 153–162. [CrossRef]
81. Fabiano, M.; Pusceddu, A.; Dell'Anno, A.; Armeni, M.; Vanucci, S.; Lampitt, R.S.; Wolff, G.A.; Danovaro, R. Fluxes of Phytopigments and Labile Organic Matter to the Deep Ocean in the NE Atlantic Ocean. *Prog. Oceanogr.* **2001**, *50*, 89–104. [CrossRef]
82. Bligh, E.G.; Dyer, W.J. A Rapid Method of Total Lipid Extraction and Purification. *Can. J. Biochem. Physiol.* **1959**, *37*, 911–917. [CrossRef]
83. Marsh, J.B.; Weinstein, D.B. Simple Charring Method for Determination of Lipids. *J. Lipid Res.* **1966**, *7*, 574–576. [CrossRef]
84. Danovaro, R.; Fabiano, M.; Della Croce, N. Labile Organic Matter and Microbial Biomasses in Deep-Sea Sediments (Eastern Mediterranean Sea). *Deep Sea Res. Part I Oceanogr. Res. Pap.* **1993**, *40*, 953–965. [CrossRef]
85. Fabiano, M.; Chiantore, M.; Povero, P.; Cattaneo-Vietti, R.; Pusceddu, A.; Misic, C.; Albertelli, G. Short-Term Variations in Particulate Matter Flux in Terra Nova Bay, Ross Sea. *Antarct. Sci.* **1997**, *9*, 143–149. [CrossRef]
86. Tselepides, A.; Polychronaki, T.; Marrale, D.; Akoumianaki, I.; Dell'Anno, A.; Pusceddu, A.; Danovaro, R. Organic Matter Composition of the Continental Shelf and Bathyal Sediments of the Cretan Sea (NE Mediterranean). *Prog. Oceanogr.* **2000**, *46*, 311–344. [CrossRef]
87. Cividanes, S.; Incera, M.; López, J. Temporal Variability in the Biochemical Composition of Sedimentary Organic Matter in an Intertidal Flat of the Galician Coast (NW Spain). *Oceanol. Acta* **2002**, *25*, 1–12. [CrossRef]
88. Dell'Anno, A.; Mei, M.L.; Pusceddu, A.; Danovaro, R. Assessing the Trophic State and Eutrophication of Coastal Marine Systems: A New Approach Based on the Biochemical Composition of Sediment Organic Matter. *Mar. Pollut. Bull.* **2002**, *44*, 611–622. [CrossRef] [PubMed]
89. Pusceddu, A.; Bianchelli, S.; Canals, M.; Sanchez-Vidal, A.; De Madron, X.D.; Heussner, S.; Lykousis, V.; de Stigter, H.; Trincardi, F.; Danovaro, R. Organic Matter in Sediments of Canyons and Open Slopes of the Portuguese, Catalan, Southern Adriatic and Cretan Sea Margins. *Deep Sea Res. Part I Oceanogr. Res. Pap.* **2010**, *57*, 441–457. [CrossRef]
90. Nardelli, M.P. *Response of Benthic Foraminifera to Pollution through Experimental and In Situ Studies: Advances in Biological Aspects and Tools for Future Application in Biomonitoring*; Università Politecnica delle Marche: Ancona, Italy, 2012.
91. Sabbatini, A.; Bonatto, S.; Gooday, A.J.; Morigi, C.; Pancotti, I.; Pucci, F.; Negri, A. Modern Benthic Foraminifers at Northern Shallow Sites of Adriatic Sea and Soft-Walled, Monothalamous Taxa: A Brief Overview. *Micropaleontology* **2010**, *56*, 359–376. [CrossRef]
92. Sabbatini, A.; Bonatto, S.; Bianchelli, S.; Pusceddu, A.; Danovaro, R.; Negri, A. Foraminiferal Assemblages and Trophic State in Coastal Sediments of the Adriatic Sea. *J. Mar. Syst.* **2012**, *105–108*, 163–174. [CrossRef]
93. Murray, J.W.; Bowser, S.S. Mortality, Protoplasm Decay Rate, and Reliability of Staining Techniques to Recognize 'Living'Foraminifera: A Review. *J. Foraminifer. Res.* **2000**, *30*, 66–70. [CrossRef]
94. Bernhard, J.M. Distinguishing Live from Dead Foraminifera: Methods Review and Proper Applications. *Micropaleontology* **2000**, *46*, 38–46.
95. Loeblich, A.R.; Tappan, H.N. Studies of Arctic Foraminifera. *Smithson. Misc. Collect.* **1953**, *121*, 150.
96. Seidenkrantz, M.-S. Cassidulina Teretis Tappan and Cassidulina Neoteretis New Species (Foraminifera): Stratigraphic Markers for Deep Sea and Outer Shelf Areas. *J. Micropalaeontol.* **1995**, *14*, 145–157. [CrossRef]
97. Wollenburg, J.E.; Mackensen, A. Living Benthic Foraminifers from the Central Arctic Ocean: Faunal Composition, Standing Stock and Diversity. *Mar. Micropaleontol.* **1998**, *34*, 153–185. [CrossRef]
98. Wollenburg, J.E.; Mackensen, A. On the Vertical Distribution of Living (Rose Bengal Stained) Benthic Foraminifers in the Arctic Ocean. *J. Foraminifer. Res.* **1998**, *28*, 268–285. [CrossRef]
99. Wollenburg, J.E.; Mackensen, A. The Ecology and Distribution of Benthic Foraminifera at the Håkon Mosby Mud Volcano (SW Barents Sea Slope). *Deep Sea Res. Part I Oceanogr. Res. Pap.* **2009**, *56*, 1336–1370. [CrossRef]
100. Majewski, W.; Zajaczkowski, M. Benthic Foraminifera in Adventfjorden, Svalbard: Last 50 Years of Local Hydrographic Changes. *J. Foraminifer. Res.* **2007**, *37*, 107–124. [CrossRef]
101. Gooday, A.J.; Bowser, S.S.; Cedhagen, T.; Cornelius, N.; Hald, M.; Korsun, S.; Pawlowski, J. Monothalamous Foraminiferans and Gromiids (Protista) from Western Svalbard: A Preliminary Survey. *Mar. Biol. Res.* **2005**, *1*, 290–312. [CrossRef]
102. Gooday, A.J.; Malzone, M.G.; Bett, B.J.; Lamont, P.A. Decadal-Scale Changes in Shallow-Infaunal Foraminiferal Assemblages at the Porcupine Abyssal Plain, NE Atlantic. *Deep Sea Res. Part II Top. Stud. Oceanogr.* **2010**, *57*, 1362–1382. [CrossRef]
103. Majewski, W.; Pawłowski, J.; Zajączkowski, M. Monothalamous Foraminifera from West Spitsbergen Fjords, Svalbard: A Brief Overview. *Pol. Polar Res.* **2005**, *26*, 269–285.

104. Sabbatini, A.; Nardelli, M.P.; Morigi, C.; Negri, A. Contribution of Soft-Shelled Monothalamous Taxa to Foraminiferal Assemblages in the Adriatic Sea. *Acta Protozool.* **2013**, *52*.
105. Pielou, E.C. *Ecological Diversity*; John Wiley & Sons: Hoboken, NJ, USA, 1975.
106. Hammer, Ø.; Harper, D.A.; Ryan, P.D. PAST: Paleontological Statistics Software Package for Education and Data Analysis. *Palaeontol. Electron.* **2001**, *4*, 9.
107. Jorissen, F.J.; de Stigter, H.C.; Widmark, J.G.V. A Conceptual Model Explaining Benthic Foraminiferal Microhabitats. *Mar. Micropaleontol.* **1995**, *26*, 3–15. [CrossRef]
108. McArdle, B.H.; Anderson, M.J. Fitting Multivariate Models to Community Data: A Comment on Distance-Based Redundancy Analysis. *Ecology* **2001**, *82*, 290–297. [CrossRef]
109. Clarke, K.R.; Warwick, R.M. A Further Biodiversity Index Applicable to Species Lists: Variation in Taxonomic Distinctness. *Mar. Ecol. Prog. Ser.* **2001**, *216*, 265–278. [CrossRef]
110. Anderson, M.; Gorley, R.N.; Clarke, R.K. *Permanova + for Primer: Guide to Software and Statisticl Methods*; Primer-E Limited: Plymouth, UK, 2008; p. 218.
111. Gribble, G.W. The Diversity of Naturally Produced Organohalogens. *Chemosphere* **2003**, *52*, 289–297. [CrossRef] [PubMed]
112. Thomson, J.; Croudace, I.W.; Rothwell, R.G. A Geochemical Application of the ITRAX Scanner to a Sediment Core Containing Eastern Mediterranean Sapropel Units. *Geol. Soc. Lond. Spec. Publ.* **2006**, *267*, 65–77. [CrossRef]
113. Passier, H.F.; Middelburg, J.J.; de Lange, G.J.; Böttcher, M.E. Modes of Sapropel Formation in the Eastern Mediterranean: Some Constraints Based on Pyrite Properties. *Mar. Geol.* **1999**, *153*, 199–219. [CrossRef]
114. Lucchi, R.G.; Rebesco, M.; Camerlenghi, A.; Busetti, M.; Tomadin, L.; Villa, G.; Persico, D.; Morigi, C.; Bonci, M.C.; Giorgetti, G. Mid-Late Pleistocene Glacimarine Sedimentary Processes of a High-Latitude, Deep-Sea Sediment Drift (Antarctic Peninsula Pacific Margin). *Mar. Geol.* **2002**, *189*, 343–370. [CrossRef]
115. Lucchi, R.G.; Camerlenghi, A.; Rebesco, M.; Colmenero-Hidalgo, E.; Sierro, F.J.; Sagnotti, L.; Urgeles, R.; Melis, R.; Morigi, C.; Bárcena, M.-A.; et al. Postglacial Sedimentary Processes on the Storfjorden and Kveithola Trough Mouth Fans: Significance of Extreme Glacimarine Sedimentation. *Glob. Planet. Chang.* **2013**, *111*, 309–326. [CrossRef]
116. Caricchi, C.; Lucchi, R.G.; Sagnotti, L.; Macrì, P.; Morigi, C.; Melis, R.; Caffau, M.; Rebesco, M.; Hanebuth, T.J. Paleomagnetism and Rock Magnetism from Sediments along a Continental Shelf-to-Slope Transect in the NW Barents Sea: Implications for Geomagnetic and Depositional Changes during the Past 15 Thousand Years. *Glob. Planet. Chang.* **2018**, *160*, 10–27. [CrossRef]
117. Renaud, P.E.; Morata, N.; Carroll, M.L.; Denisenko, S.G.; Reigstad, M. Pelagic–Benthic Coupling in the Western Barents Sea: Processes and Time Scales. *Deep Sea Res. Part II Top. Stud. Oceanogr.* **2008**, *55*, 2372–2380. [CrossRef]
118. Wassmann, P.; Reigstad, M. Future Arctic Ocean Seasonal Ice Zones and Implications for Pelagic-Benthic Coupling. *Oceanography* **2011**, *24*, 220–231. [CrossRef]
119. Søreide, J.E.; Carroll, M.L.; Hop, H.; Ambrose, W.G., Jr.; Hegseth, E.N.; Falk-Petersen, S. Sympagic-Pelagic-Benthic Coupling in Arctic and Atlantic Waters around Svalbard Revealed by Stable Isotopic and Fatty Acid Tracers. *Mar. Biol. Res.* **2013**, *9*, 831–850. [CrossRef]
120. Wlodarska-Kowalczuk, M.; Pearson, T.H.; Kendall, M.A. Benthic Response to Chronic Natural Physical Disturbance by Glacial Sedimentation in an Arctic Fjord. *Mar. Ecol. Prog. Ser.* **2005**, *303*, 31–41. [CrossRef]
121. Kędra, M.; Renaud, P.E.; Andrade, H.; Goszczko, I.; Ambrose, W.G. Benthic Community Structure, Diversity, and Productivity in the Shallow Barents Sea Bank (Svalbard Bank). *Mar. Biol.* **2013**, *160*, 805–819. [CrossRef] [PubMed]
122. Ślubowska-Woldengen, M.; Koç, N.; Rasmussen, T.L.; Klitgaard-Kristensen, D.; Hald, M.; Jennings, A.E. Time-Slice Reconstructions of Ocean Circulation Changes on the Continental Shelf in the Nordic and Barents Seas during the Last 16,000 Cal Yr BP. *Quat. Sci. Rev.* **2008**, *27*, 1476–1492. [CrossRef]
123. Grémare, A.; Medernach, L.; DeBovee, F.; Amouroux, J.M.; Vétion, G.; Albert, P. Relationships between Sedimentary Organics and Benthic Meiofauna on the Continental Shelf and the Upper Slope of the Gulf of Lions (NW Mediterranean). *Mar. Ecol. Prog. Ser.* **2002**, *234*, 85–94. [CrossRef]
124. Schubert, C.J.; Calvert, S.E. Nitrogen and Carbon Isotopic Composition of Marine and Terrestrial Organic Matter in Arctic Ocean Sediments:: Implications for Nutrient Utilization and Organic Matter Composition. *Deep Sea Res. Part I Oceanogr. Res. Pap.* **2001**, *48*, 789–810. [CrossRef]
125. Goñi, M.A.; Teixeira, M.J.; Perkey, D.W. Sources and Distribution of Organic Matter in a River-Dominated Estuary (Winyah Bay, SC, USA). *Estuar. Coast. Shelf Sci.* **2003**, *57*, 1023–1048. [CrossRef]
126. Meyers, P.A. Preservation of Elemental and Isotopic Source Identification of Sedimentary Organic Matter. *Chem. Geol.* **1994**, *114*, 289–302. [CrossRef]
127. Knies, J.; Martinez, P. Organic Matter Sedimentation in the Western Barents Sea Region: Terrestrial and Marine Contribution Based on Isotopic Composition and Organic Nitrogen Content. *Nor. J. Geol./Nor. Geol. Foren.* **2009**, *89*, 79–89.
128. Pusceddu, A.; Bianchelli, S.; Gambi, C.; Danovaro, R. Assessment of Benthic Trophic Status of Marine Coastal Ecosystems: Significance of Meiofaunal Rare Taxa. *Estuar. Coast. Shelf Sci.* **2011**, *93*, 420–430. [CrossRef]
129. Bianchelli, S.; Gambi, C.; Pusceddu, A.; Danovaro, R. Trophic Conditions and Meiofaunal Assemblages in the Bari Canyon and the Adjacent Open Slope (Adriatic Sea). *Chem. Ecol.* **2008**, *24*, 101–109. [CrossRef]

130. Pusceddu, A.; Dell'Anno, A.; Danovaro, R.; Manini, E.; Sara, G.; Fabiano, M. Enzymatically Hydrolyzable Protein and Carbohydrate Sedimentary Pools as Indicators of the Trophic State of Detritus Sink Systems: A Case Study in a Mediterranean Coastal Lagoon. *Estuaries* **2003**, *26*, 641–650. [CrossRef]
131. Lantzsch, H.; Hanebuth, T.J.J.; Horry, J.; Grave, M.; Rebesco, M.; Schwenk, T. Deglacial to Holocene History of Ice-Sheet Retreat and Bottom Current Strength on the Western Barents Sea Shelf. *Quat. Sci. Rev.* **2017**, *173*, 40–57. [CrossRef]
132. Caridi, F.; Sabbatini, A.; Morigi, C.; Dell'Anno, A.; Negri, A.; Lucchi, R.G. Patterns and Environmental Drivers of Diversity and Community Composition of Macrofauna in the Kveithola Trough (NW Barents Sea). *J. Sea Res.* **2019**, *153*, 101780. [CrossRef]
133. Morigi, C.; Jorissen, F.J.; Gervais, A.; Guichard, S.; Borsetti, A.M. Benthic Foraminiferal Faunas in Surface Sediments off NW Africa: Relationship with Organic Flux to the Ocean Floor. *J. Foraminifer. Res.* **2001**, *31*, 350–368. [CrossRef]
134. Fontanier, C.; Jorissen, F.J.; Chaillou, G.; Anschutz, P.; Grémare, A.; Griveaud, C. Live Foraminiferal Faunas from a 2800 m Deep Lower Canyon Station from the Bay of Biscay: Faunal Response to Focusing of Refractory Organic Matter. *Deep Sea Res. Part I Oceanogr. Res. Pap.* **2005**, *52*, 1189–1227. [CrossRef]
135. Gooday, A.J. A Response by Benthic Foraminifera to the Deposition of Phytodetritus in the Deep Sea. *Nature* **1988**, *332*, 70–73. [CrossRef]
136. Gooday, A.J.; Turley, C.M. Responses by Benthic Organisms to Inputs of Organic Material to the Ocean Floor: A Review. *Philos. Trans. R. Soc. London. Ser. A Math. Phys. Sci.* **1990**, *331*, 119–138.
137. Gooday, A.J.; Rathburn, A.E. Temporal Variability in Living Deep-Sea Benthic Foraminifera: A Review. *Earth-Sci. Rev.* **1999**, *46*, 187–212. [CrossRef]
138. Gooday, A.J. Biological Responses to Seasonally Varying Fluxes of Organic Matter to the Ocean Floor: A Review. *J. Oceanogr.* **2002**, *58*, 305–332. [CrossRef]
139. Kitazato, H.; Shirayama, Y.; Nakatsuka, T.; Fujiwara, S.; Shimanaga, M.; Kato, Y.; Okada, Y.; Kanda, J.; Yamaoka, A.; Masuzawa, T. Seasonal Phytodetritus Deposition and Responses of Bathyal Benthic Foraminiferal Populations in Sagami Bay, Japan: Preliminary Results from "Project Sagami 1996–1999". *Mar. Micropaleontol.* **2000**, *40*, 135–149. [CrossRef]
140. Licari, L.N. Communities and Microhabitats of Living Benthic Foraminifera from the Tropical East Atlantic: Impact of Different Productivity Regimes. *J. Foraminifer. Res.* **2003**, *33*, 10–31. [CrossRef]
141. Saher, M.; Kristensen, D.K.; Hald, M.; Pavlova, O.; Jørgensen, L.L. Changes in Distribution of Calcareous Benthic Foraminifera in the Central Barents Sea between the Periods 1965–1992 and 2005–2006. *Glob. Planet. Chang.* **2012**, *98–99*, 81–96. [CrossRef]
142. Mackensen, A.; Sejrup, H.P.; Jansen, E. The Distribution of Living Benthic Foraminifera on the Continental Slope and Rise off Southwest Norway. *Mar. Micropaleontol.* **1985**, *9*, 275–306. [CrossRef]
143. Corliss, B.H.; Chen, C. Morphotype Patterns of Norwegian Sea Deep-Sea Benthic Foraminifera and Ecological Implications. *Geology* **1988**, *16*, 716–719. [CrossRef]
144. Linke, P.; Lutze, G.F. Microhabitat Preferences of Benthic Foraminifera—A Static Concept or a Dynamic Adaptation to Optimize Food Acquisition? *Mar. Micropaleontol.* **1993**, *20*, 215–234. [CrossRef]
145. Yak, L.P.; Solheim, A. Late-and Postglacial Environments in the Northern Barents Sea West of Franz Josef Land. *Polar Res.* **1994**, *13*, 197–207. [CrossRef]
146. Polyak, L.; Korsun, S.; Febo, L.A.; Stanovoy, V.; Khusid, T.; Hald, M.; Paulsen, B.E.; Lubinski, D.J. Benthic Foraminiferal Assemblages from the Southern Kara Sea, a River-Influenced Arctic Marine Environment. *J. Foraminifer. Res.* **2002**, *32*, 252–273. [CrossRef]
147. Wollenburg, J.E.; Kuhnt, W. The Response of Benthic Foraminifers to Carbon Flux and Primary Production in the Arctic Ocean. *Mar. Micropaleontol.* **2000**, *40*, 189–231. [CrossRef]
148. Rytter, F. Modern Distribution of Benthic Foraminifera on the North Icelandic Shelf and Slope. *J. Foraminifer. Res.* **2002**, *32*, 217–244. [CrossRef]
149. Wollenburg, J.E.; Knies, J.; Mackensen, A. High-Resolution Paleoproductivity Fluctuations during the Past 24 Kyr as Indicated by Benthic Foraminifera in the Marginal Arctic Ocean. *Palaeogeogr. Palaeoclimatol. Palaeoecol.* **2004**, *204*, 209–238. [CrossRef]
150. Wollenburg, J.E.; Kuhnt, W.; Mackensen, A. Changes in Arctic Ocean Paleoproductivity and Hydrography during the Last 145 Kyr: The Benthic Foraminiferal Record. *Paleoceanography* **2001**, *16*, 65–77. [CrossRef]
151. Husum, K.; Hald, M. Early Holocene Cooling Events in Malangenfjord and the Adjoining Shelf, North-East Norwegian Sea. *Polar Res.* **2002**, *21*, 267–274. [CrossRef]
152. Husum, K.; Hald, M. Modern Foraminiferal Distribution in the Subarctic Malangen Fjord and Adjoining Shelf, Northern Norway. *J. Foraminifer. Res.* **2004**, *34*, 34–48. [CrossRef]
153. Ernst, S.; van der Zwaan, B. Effects of Experimentally Induced Raised Levels of Organic Flux and Oxygen Depletion on a Continental Slope Benthic Foraminiferal Community. *Deep Sea Res. Part I Oceanogr. Res. Pap.* **2004**, *51*, 1709–1739. [CrossRef]
154. Caulle, C.; Koho, K.A.; Mojtahid, M.; Reichart, G.J.; Jorissen, F.J. Live (Rose Bengal Stained) Foraminiferal Faunas from the Northern Arabian Sea: Faunal Succession within and below the OMZ. *Biogeosciences* **2014**, *11*, 1155–1175. [CrossRef]
155. Ekeroth, N.; Blomqvist, S.; Hall, P.O. Nutrient Fluxes from Reduced Baltic Sea Sediment: Effects of Oxygenation and Macrobenthos. *Mar. Ecol. Prog. Ser.* **2016**, *544*, 77–92. [CrossRef]
156. Keil, R.G.; Montluçon, D.B.; Prahl, F.G.; Hedges, J.I. Sorptive Preservation of Labile Organic Matter in Marine Sediments. *Nature* **1994**, *370*, 549–552. [CrossRef]

157. Knicker, H.; Hatcher, P.G. Survival of Protein in an Organic-Rich Sediment: Possible Protection by Encapsulation in Organic Matter. *Naturwissenschaften* **1997**, *84*, 231–234. [CrossRef]
158. Rohling, E.J.; Marino, G.; Grant, K.M. Mediterranean Climate and Oceanography, and the Periodic Development of Anoxic Events (Sapropels). *Earth-Sci. Rev.* **2015**, *143*, 62–97. [CrossRef]
159. Lourens, L.J. Revised Tuning of Ocean Drilling Program Site 964 and KC01B (Mediterranean) and Implications for the Δ18O, Tephra, Calcareous Nannofossil, and Geomagnetic Reversal Chronologies of the Past 1.1 Myr. *Paleoceanography* **2004**, *19*, PA3010. [CrossRef]
160. Morigi, C. Benthic Environmental Changes in the Eastern Mediterranean Sea during Sapropel S5 Deposition. *Palaeogeogr. Palaeoclimatol. Palaeoecol.* **2009**, *273*, 258–271. [CrossRef]
161. Schmidt, D.N.; Renaud, S.; Bollmann, J. Response of Planktic Foraminiferal Size to Late Quaternary Climate Change. *Paleoceanography* **2003**, *18*. [CrossRef]
162. Richter, R. Aktuopaläontologie Und Paläobiologie, Eine Abgrenzung. *Senckenbergiana* **1928**, *10*, 285–292.